Published October 1, 1989

Calcium Signals Recorded from Two New Purpurate Indicators Inside Frog Cut Twitch Fibers

AKIHIKO HIROTA, W. KNOX CHANDLER, PHILIP L. SOUTHWICK, and ALAN S. WAGGONER

From the Department of Cellular and Molecular Physiology, Yale University School of Medicine, New Haven, Connecticut 06510; Department of Chemistry and Center for Fluorescence Research, Carnegie Mellon University, Pittsburgh, Pennsylvania 15213

ABSTRACT Two new Ca indicators, purpurate-3,3'diacetic acid (PDAA) and 1,1'-dimethylpurpurate-3,3'diacetic acid (DMPDAA), were synthesized and used to measure Ca transients in frog cut muscle fibers. These indicators are analogues of the purpurate components of murexide and tetramethylmurexide, in which two acetate groups have been incorporated into each molecule to render it membrane impermeant. The apparent dissociation constant for Ca is 0.95 mM for PDAA and 0.78 mM for DMPDAA. One of the indicators was introduced into a cut fiber, which was mounted in a double Vaseline-gap chamber, by diffusion from the end-pool solutions. The time course of indicator concentration, monitored optically in the middle of the fiber in the central-pool region, suggests that 19% of the PDAA or 27% of the DMPDAA became bound or sequestered inside the fiber. In resting fibers, the absorbance spectrum of either indicator was well fitted by the indicator's [Ca] = 0 mM cuvette absorbance spectrum, which is consistent with the idea that PDAA and DMPDAA do not enter the sarcoplasmic reticulum as tetramethylmurexide appears to be able to do (Maylie, J., M. Irving, N.L. Sizto, G. Boyarsky, and W. K. Chandler. 1987. *Journal of General Physiology.* 89:145–176). After an action potential, the absorbance of either indicator underwent a rapid and transient change that returned to the prestimulus baseline within 100–200 ms. The amplitude of this change had a wavelength dependence that matched the indicator's Ca-difference spectrum. The average amplitude of peak free [Ca] was 21 μM (PDAA or DMPDAA) if all the indicator inside a fiber was able to react with Ca as in cuvette calibrations, and was 26 (PDAA) or 28 μM (DMPDAA) if only freely diffusible indicator could so react. These results suggest that PDAA and DMPDAA are the first Ca indicators that provide a reliable estimate of both the amplitude and time course of (the spatial average of) free [Ca] in a twitch muscle fiber after an action potential.

Address reprint requests to Dr. W. Knox Chandler, Department of Cellular and Molecular Physiology, 333 Cedar Street, P.O. Box 3333, New Haven, CT 06510-8026.

Dr. Hirota's present address is Department of Physiology, Tokyo Medical and Dental University, 5-45, Yushima, 1-Chome, Bunkyo-ku, Tokyo 113, Japan.

J. GEN. PHYSIOL. © The Rockefeller University Press · 0022-1295/89/10/0597/35 $2.00
Volume 94 October 1989 597–631

INTRODUCTION

After an action potential in a skeletal muscle fiber, there is a transient increase in myoplasmic free [Ca] that activates the contractile machinery. This increase can be measured with an indicator that undergoes a change in its optical properties when it complexes Ca. The first reproducible measurements of this kind were made by Ashley and Ridgway (1970) on barnacle muscle fibers and by Rudel and Taylor (1973), Miledi et al. (1977), and Blinks et al. (1978) on frog twitch fibers.

Although the existence of a myoplasmic [Ca] transient is now well established, its magnitude remains in doubt. The first estimates of peak free [Ca] after a single action potential in frog muscle were in the low micromolar range, and the exact value depended on which particular indicator was used. For example, 5.25–8 μM was obtained with arsenazo III (Miledi et al., 1977, 1982), 2.2–2.9 μM with antipyrylazo III (Baylor et al., 1982*b*, 1983*b*), and 0.5–0.6 μM with azo1 (Hollingworth and Baylor, 1986). Recent work indicates that a substantial fraction of many of the Ca indicators used in muscle becomes bound or sequestered once the indicator is introduced into a fiber (Baylor et al., 1986; Maylie et al., 1987*a–c*). Consequently, any estimate of free [Ca] depends on whether these immobilized indicator molecules are able to react with Ca in the same manner as indicator molecules react in cuvette calibrations.

Recent experiments (Maylie et al., 1987*c*), carried out on cut twitch fibers (Hille and Cambell, 1976) mounted in a double Vaseline-gap chamber (Kovacs et al., 1983), illustrate this kind of uncertainty in the estimation of free [Ca]. After its addition to the end-pool solutions, antipyrylazo III was found to diffuse into the optical recording site in the middle of a fiber in the central-pool region where, after ~1 h, its concentration exceeded that in the end pools. This concentrating effect provides clear evidence that some of the indicator molecules were bound or sequestered inside the fiber. The time course of indicator appearance was analyzed on the assumptions (*a*) that the movement of free, or unbound, indicator along the fiber axis was described by the standard one-dimensional diffusion equation, (*b*) that the concentration of bound or sequestered indicator was proportional to the concentration of free indicator, and (*c*) that the constant of proportionality did not change during an experiment. According to this analysis, approximately two-thirds of the antipyrylazo III inside a fiber was bound or sequestered. The peak increase in free [Ca] after an action potential was estimated by comparing the change in indicator absorbance inside a fiber with that determined in cuvette calibrations. If all the indicator inside a fiber was able to react with Ca in the same manner as in a cuvette, the peak amplitude of free [Ca] was 3 μM. If only freely diffusible indicator could so react, the peak amplitude was 43 μM. These two estimates probably bracket the actual calibration inside a fiber. The 13-fold difference between them is due to the predominant stoichiometry of the Ca:indicator complex being 1:2 (Palade and Vergara, 1981; Rios and Schneider, 1981) and to the nonlinearity in the relation between indicator absorbance and free [Ca].

To help resolve this uncertainty in the estimation of the amplitude of myoplasmic free [Ca] signals, Maylie et al. (1987*a*) carried out experiments using a chemically different kind of indicator, murexide (Jobsis and O'Connor, 1966) or tetramethylmurexide (Ohnishi, 1978). Similar results were obtained in preliminary experiments

with both indicators so that one of them, tetramethylmurexide, was used for the figures and tables in their article. There were four main results: (*a*) The analysis of the time course of tetramethylmurexide diffusion in cut fibers indicated that, on average, 0.27 of the indicator was bound or sequestered. (*b*) The wavelength dependence of indicator absorbance in resting fibers indicated that 0.11–0.15 of the indicator was complexed with Ca. (*c*) After action potential stimulation, the indicator underwent an early change in absorbance, due to Ca complexation produced by the myoplasmic Ca transient. This signal reversed direction within 10–20 ms and then reached a steady level that was maintained for at least 8 s. The amplitude of this reversed steady signal was about one-half that of the peak early change. (*d*) The amplitude of the early signal varied linearly with indicator concentration with a slope that corresponded to an increase in peak free [Ca] of 15–20 μM.

Two of these findings had not been observed with either arsenazo III (Maylie et al., 1987*b*) or antipyrylazo III (Maylie et al., 1987*c*): (*b*) the presence of significant Ca complexation by indicator inside resting fibers, in spite of tetramethylmurexide's low affinity for Ca (its dissociation constant, K_D, is 2.6 mM, Maylie et al., 1987*a*) and (*c*) the presence of a reversed maintained signal after stimulation. Maylie et al. (1987*a*) suggested that tetramethylmurexide, but neither arsenazo III nor antipyrylazo III, was able to enter the sarcoplasmic reticulum (SR) of cut fibers, similar to the way in which it can enter isolated SR vesicles (Ohnishi, 1979; Ogawa et al., 1980). This idea is plausible since the single negative charge on tetramethylmurexide, shared among four oxygens, is delocalized and consequently would not be expected to render the molecule membrane impermeant (Sims et al., 1974). If tetramethylmurexide is able to enter the SR, some of the indicator should become complexed with Ca (finding *b*) and, after activity, some of these complexes might dissociate as Ca moves from inside the SR into the myoplasm (reversed maintained signal in finding *c*).

To test the idea that the murexide indicators can cross the SR membrane, we synthesized two new compounds: purpurate-3,3′diacetic acid (PDAA), an analogue of murexide, and 1,1′-dimethylpurpurate-3,3′diacetic acid (DMPDAA), an analogue of tetramethylmurexide. (These compounds are called "purpurate" instead of "murexide" since murexide represents ammonium purpurate—and tetramethylmurexide, ammonium tetramethylpurpurate—and it is the purpurate molecule that is the Ca indicator; in the rest of this article, purpurate will be used to denote the Ca indicator.) Each of the analogues contains two acetic acid groups. At neutral pH, both groups are expected to be ionized and the resulting localized charges should make the molecule membrane impermeant (Sims et al., 1974).

Absorbance measurements made with PDAA and DMPDAA inside cut muscle fibers showed that the amount of Ca complexed by the indicator at rest was not statistically significant (in contrast to finding *b* with tetramethylpurpurate) and that, within the accuracy of the measurements, there was little or no reversed maintained signal (in contrast to finding *c* with tetramethylpurpurate). These findings are consistent with the idea that tetramethylpurpurate can enter the SR but that PDAA and DMPDAA are mostly or extirely excluded. After action potential stimulation, the peak amplitude of the absorbance change of PDAA and DMPDAA varied approximately linearly with indicator concentration with a slope that corresponds to an

increase in myoplasmic free [Ca] of 10–30 μM, which is similar to the results obtained with tetramethylpurpurate (Maylie et al., 1987*a*, the myoplasmic component). This article describes these and other results obtained in frog cut muscle fibers with these two new Ca indicators.

A preliminary report of some of the results obtained with DMPDAA has been presented to the Biophysical Society (Hirota et al., 1988).

METHODS

The frog muscle experiments were carried out at Yale University School of Medicine with the method described in Irving et al. (1987). Cut twitch fibers (Hille and Campbell, 1976) were prepared from semitendinosus muscles of cold-adapted *Rana temporaria* and were mounted in a double Vaseline-gap chamber, similar to that used by Kovacs et al. (1983). The striation spacing was 3.8–4.3 μm. The end-pool segments of the fiber were permeabilized by a 2-min exposure to a 0.01% saponin solution followed by a thorough rinse. Then, a potassium glutamate solution containing ATP and creatine phosphate was introduced into the end pools and Ringer's solution was put into the central pool. The composition of these solutions is given in Table I of Irving et al. (1987). The end-pool solutions contained 0.1 mM EGTA, a concentration that is not expected to alter either the amplitude or time course of the myoplasmic Ca signals (Palade and Vergara, 1982). The central-pool solution was maintained at 16.0 ± 0.2°C, and the holding potential, measured in the potential-measuring end pool, was maintained at −90 mV. The stimulation rate was ≦1/min.

Transmitted light intensities at three different wavelengths and two planes of linear polarization were measured with the apparatus described in Irving et al. (1987), with mode 1 recording. 570- and 690-nm interference filters with a 30-nm bandpass were used in the λ_2 and λ_3 positions, respectively; filters with a 10-nm bandpass were used in the λ_1 position (Fig. 2 in Irving et al., 1987). Details concerning the processing of optical signals are described in that paper and in Maylie et al. (1987*a–c*). The measurements of transmitted light intensities have been expressed in terms of absorbance and are given at 1:2 averages of (absorbance of light linearly polarized along the fiber axis, i.e., 0° light):(absorbance of light linearly polarized perpendicular to the fiber axis, i.e., 90° light).

The concentration of indicator, c, at the optical recording site was estimated from the value of indicator-related absorbance, $A(\lambda)$, with Beer's law,

$$A(\lambda) = \epsilon(\lambda)cl, \tag{1}$$

as described in Maylie et al. (1987*b*). $\epsilon(\lambda)$ represents the molar extinction coefficient of the indicator, which was assumed to be independent of indicator concentration, and λ represents the wavelength of light. l, the optical path length, was estimated on the assumption that the indicator is confined to myoplasmic water. l was taken to be equal to the product of the fiber diameter, determined each time by interpolation between measurements made during the experiment, and the factor 0.7, estimated as the fraction of muscle volume that is occupied by myoplasmic water (Baylor et al., 1983*a*). Since the cross section of a fiber becomes very nearly circular when the fiber is stretched to a striation spacing of 3.5 μm or more (Blinks, 1965), the horizontal diameter measured in the microscope, which was used to estimate l, should be approximately equal to the vertical diameter that spans the optical path.

The statistical significance of a difference between two sets of results was determined with the two-tailed t test; if $P > 0.05$, the difference was considered to be not significant.

Determination of Free [Ca]

In this article, myoplasmic [Ca] transients were measured with the two new purpurate indicators PDAA and DMPDAA that were synthesized at Carnegie Mellon University. As indicated

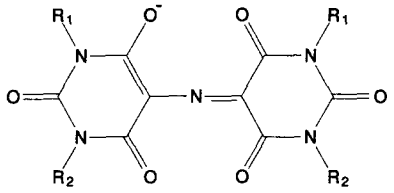

FIGURE 1. Chemical structure of the purpurate indicators. For purpurate (murexide), $R_1 = R_2 = H$; for tetramethylpurpurate (tetramethylmurexide), $R_1 = R_2 = CH_3$; for purpurate-3,3'diacetic acid (PDAA), $R_1 = H$ and $R_2 = CH_2COOH$; for 1,1'-dimethylpurpurate-3,3'diacetic acid (DMPDAA), $R_1 = CH_3$ and $R_2 = CH_2COOH$. The molecular weights of the ionized molecules at neutral pH are 266 for purpurate, 322 for tetramethylpurpurate, 380 for PDAA, and 408 for DMPDAA.

in Fig. 1 and its legend, PDAA and DMPDAA have the same R_1 groups as purpurate and tetramethylpurpurate, respectively, but acetic acid groups in the R_2 positions. The synthesis of the potassium salt of PDAA is described in Southwick and Waggoner (1989) and that of the ammonium salt of DMPDAA is described below.

The absorbance of indicator in calibration solutions was measured with 1-cm path-length cuvettes placed inside a spectrophotometer (model Lambda 3B; Perkin-Elmer Corp., Norwalk, CT; nominal bandpass, 1 nm) in which the temperature was controlled at 16°C. The calibration solutions contained 25–50 μM indicator, 150 mM KCl, 10 mM PIPES, 0–2 mM $MgCl_2$, and 0–10 mM $CaCl_2$.

Fig. 2 *A* shows the wavelength dependence of PDAA absorbance in calibration solutions that contained 0, 0.5, 1.5, 4.0, and 10.0 mM total [Ca]; the concentration of PDAA was 26 μM, [Mg] = 0 mM, and pH 7.0. The curves intersect at 511 nm, the isosbestic wavelength for

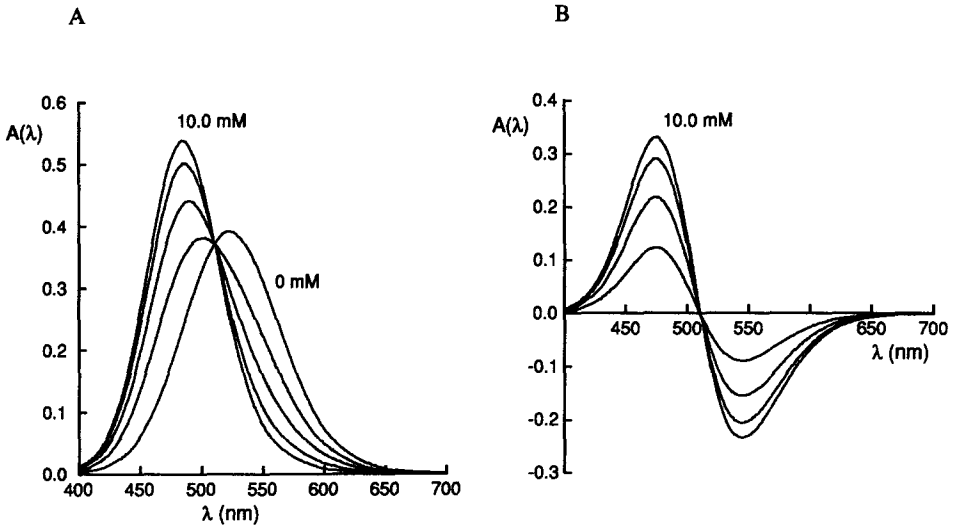

FIGURE 2. Effect of Ca concentration on the absorbance of PDAA. (*A*) The absorbance of calibration solutions that contained 0, 0.5, 1.5, 4.0, or 10.0 mM $CaCl_2$ as well as 26 μM PDAA, 150 mM KCl, and 10 mM PIPES, pH 7.0. The 0 mM Ca solution also contained 0.1 mM K_2EGTA. The 0 and 10.0 mM Ca curves are labeled; the amplitude of the 0.5, 1.5, and 4.0 mM curves increased progressively with increasing Ca. (*B*) Ca-difference spectra obtained by subtraction of the 0 mM Ca curve in *A* from the 0.5, 1.5, 4.0, and 10.0 mM curves. The amplitude of the curves progressively increased with increasing Ca; the 10.0 mM Ca-difference curve is labeled. The measurements were made with 1-cm path-length cuvettes.

this indicator. A similar set of curves was obtained with DMPDAA (not shown), in which the isosbestic wavelength was 516 nm. The molar extinction coefficient, $\epsilon(\lambda)$, of Ca-free PDAA was estimated from the 0 mM curve in Fig. 2 *A*. The value of $\epsilon(520)$, 1.50×10^4 $M^{-1}cm^{-1}$, was used to estimate the concentration of indicator inside a muscle fiber (cf. Maylie et al., 1987*a*). The sample of DMPDAA was probably less pure than that of PDAA (see page 605), so that the value of $\epsilon(520)$ for this indicator was assumed to be the same as that for tetramethylpurpurate, 1.58×10^4 $M^{-1}cm^{-1}$ (Maylie et al., 1987*a*, page 147).

In Fig. 2 *A*, the peak value of PDAA absorbance increased when [Ca] was increased from 0 to 10.0 mM and the position of the peak shifted almost 40 nm towards shorter wavelengths. Fig. 2 *B* shows Ca-difference spectra, obtained by subtraction of the [Ca] = 0 mM spectrum in Fig. 2 *A* from the [Ca] = 0.5–10.0 mM spectra. The Ca-difference spectrum for 10.0 mM Ca was least-squares fitted, between 400 and 700 nm, to the Ca-difference spectra for 0.5, 1.5, and 4.0 mM Ca to give three scaling constants.

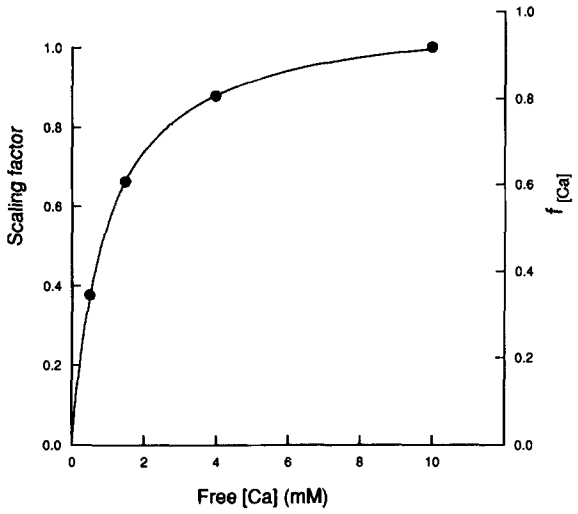

FIGURE 3. Determination of the dissociation constant of Ca and PDAA. The 10.0 mM Ca-difference curve in Fig. 2 *B* was least-squares fitted, from 400 to 700 nm, to the other Ca-difference curves. The scaling constants, including the value of unity for the 10.0 mM curve, have been plotted (left-hand ordinate) as a function of free [Ca], estimated by subtraction of indicator-bound [Ca] from total [Ca]. The curve (right-hand ordinate) shows the best least-squares fit of Eq. 1, obtained with K_D = 0.95 mM. The curve has a value of 0.916 for free [Ca] equal to that associated with the total [Ca] = 10.0 mM point.

Fig. 3 (left-hand ordinate) shows these three scaling constants, plus the value of unity that applies to the 10.0 mM Ca-difference spectrum, plotted as a function of free [Ca]. If the stoichiometry of Ca:indicator complexation is 1:1, as appears to be the case for purpurate and tetramethylpurpurate (Ohnishi, 1978; Maylie et al., 1987*a*), the fraction of indicator complexed with Ca should obey

$$f_{[Ca]} = \frac{[Ca]}{[Ca] + K_D}. \quad (2)$$

$f_{[Ca]}$ is the fraction of indicator that is complexed with Ca when the concentration of free Ca is [Ca] and K_D is the apparent dissociation constant of the indicator for Ca; free [Ca] is estimated by subtraction of indicator-bound [Ca] from total [Ca]. The theoretical curve in Fig. 3 (right-hand ordinate) shows the least-squares fit of Eq. 2 after adjustment of K_D to 0.95 mM. The curve has a value of 0.916 at the [Ca] = 10.0 mM point. Hence, according to this analy-

sis, the 10.0 mM Ca-difference spectrum in Fig. 2 *B*, divided by the product of 0.916 times the indicator concentration, gives the change in molar extinction coefficient, $\Delta\epsilon(\lambda)$, that would occur if all the indicator changed from a Ca-free to a Ca-complexed state. At 570 nm, the wavelength routinely used to monitor changes in Ca-complexation, $\Delta\epsilon(570) = 0.70 \times 10^4$ $M^{-1}cm^{-1}$ (and $\Delta\epsilon(570)/\epsilon(520) = 0.47$).

DMPDAA, studied under similar ionic conditions, gave $\Delta\epsilon(570)/\epsilon(520) = 0.53$. If $\epsilon(520)$ is assumed to be 1.58×10^4 $M^{-1}cm^{-1}$ (see page 605), the concentration of indicator used for the calibrations was 25 μM, $\Delta\epsilon(570) = 0.84 \times 10^4$ $M^{-1}cm^{-1}$, and $K_D = 0.78$ mM. On the other hand, if the sample of DMPDAA was chemically pure and $\epsilon(520) = 1 \times 10^4$ $M^{-1}cm^{-1}$ (see page 605), the concentration of indicator would be 40 μM, $\Delta\epsilon(570)$ would be 0.53×10^4 $M^{-1}cm^{-1}$, and K_D would be 0.77 mM.

Calibration measurements were carried out with PDAA, but not DMPDAA, in which free [Mg] and pH were varied (not shown). At pH 7.0, the Ca-free spectrum was the same with 0 and 2 mM [Mg], as was the Ca-difference spectrum; K_D was 0.95 mM with [Mg] = 0 mM and 0.94 mM with [Mg] = 2 mM. Thus, the Ca-indicator properties of PDAA do not appear to be sensitive to Mg at concentrations of 0–2 mM. With [Mg] = 0 mM, changes in pH in the range 6.5–7.5 had no effect on either the Ca-free spectrum or the Ca-difference spectrum that is associated with a change in all the indicator from a Ca-free to a Ca-complexed state. There was a slight effect of pH on the K_D, however; $K_D = 0.98$ mM at pH 6.5, 0.95 mM at pH 7.0, and 0.89 mM at pH 7.5.

The speed of the reaction between Ca and PDAA or DMPDAA has not been measured. It is expected to be similar to that between Ca and purpurate, for which the dissociation rate constant k_{-1} is $\geq 1.6 \times 10^5$ s^{-1} at 10°C (Geier, 1968). Since myoplasmic free [Ca] $\ll K_D$, the change in [Ca: purpurate] produced by a change in free [Ca] is expected to occur with a delay that is approximately equal to $1/k_{-1}$, which is ≤ 6 μs. Thus, purpurate should track changes in intracellular free [Ca] essentially instantaneously, and PDAA and DMPDAA are expected to do likewise.

In our cut fiber experiments, PDAA absorbance signals were measured and analyzed in the same way as the tetramethylpurpurate absorbance Ca signals described in Maylie et al. (1987*a*), with the following calibration parameters:

(*a*) $\epsilon(520) = 1.50 \times 10^4$ $M^{-1}cm^{-1}$ was used to estimate the concentration of PDAA, [PDAA], from Beer's law and the value of indicator-related absorbance measured with our 520-nm filter (10-nm bandpass).

(*b*) $\Delta\epsilon(570) = 0.70 \times 10^4$ $M^{-1}cm^{-1}$ was used to estimate changes in the concentration of Ca:PDAA complexes, Δ[Ca:PDAA], from Beer's law and the value of the change in indicator-related absorbance measured with our 570-nm filter (10-nm bandpass). $\Delta\epsilon(570) = 0.66 \times 10^4$ $M^{-1}cm^{-1}$ was used to estimate Δ[Ca:PDAA] from measurements of ΔA(570) made with our 570-nm filter (30-nm bandpass); this value of $\Delta\epsilon(570)$ was obtained by scaling the indicator-related ΔA(570) signal measured with the 10-nm band pass filter to fit that measured simultaneously with the 30-nm bandpass filter, and then dividing the scaling constant into the value of $\Delta\epsilon(570)$ for the 10-nm bandpass filter (i.e., 0.70×10^4 $M^{-1}cm^{-1}$).

(*c*) $K_D = 0.95$ mM and Eq. 2 were used to estimate free [Ca] from $f_{[Ca]} = \Delta[Ca:PDAA]/[PDAA]$; this equality requires that resting [Ca:PDAA] = 0 mM, which, within the accuracy of our measurements, appears to be the case (Fig. 6 and pages 608–609).

DMPDAA absorbance signals were analyzed in the same way as PDAA absorbance signals with (*a*) $\epsilon(520) = 1.58 \times 10^4$ $M^{-1}cm^{-1}$ (see above and page 605), (*b*) $\Delta\epsilon(570) = 0.84 \times 10^4$ $M^{-1}cm^{-1}$ (on average, the amplitude of the indicator-related $\Delta A(570)$ signal was the same with either the 10- or 30-nm bandpass filter), and (*c*) $K_D = 0.78$ mM.

If $\epsilon(520)$ for DMPDAA is 1.00×10^4 $M^{-1}cm^{-1}$ and $K_D = 0.77$ mM (see above), the values of myoplasmic free [Ca] that are reported in this article for DMPDAA should be multiplied by the ratio of the K_D's for $\epsilon(520) = 1.00 \times 10^4$ $M^{-1}cm^{-1}$ and $\epsilon(520) = 1.58 \times 10^4$ $M^{-1}cm^{-1}$,

0.77/0.78 = 0.99. This reason for this factor follows from rearranging Eq. 2 to give [Ca] = $K_D f_{[Ca]}/(1 - f_{[Ca]})$ and remembering that the estimate of $f_{[Ca]}$, which depends only on $\Delta\epsilon(570)/\epsilon(520)$, is not affected by the value used for $\epsilon(520)$. Thus, the calibration of myoplasmic free [Ca] is relatively insensitive to the value used for $\epsilon(520)$, although the estimates of the concentrations of total DMPDAA and of Ca-complexed DMPDAA are sensitive to the value of $\epsilon(520)$.

Synthesis of 1,1'-Dimethylpurpurate-3,3'Diacetic Acid Ammonium Salt

Theobromine-1-acetic acid (Fig. 4, compound 1) (Merck et al., 1922; McMillan and Wuenst, 1953) (0.48 g, 2 mmol) was dissolved in 3 ml of 4N hydrochloric acid. The solution was stirred in a 55°C bath while a solution containing potassium chlorate (0.24 g, 2 mmol) dissolved in 4 ml of hot water was added during a 1.5-h period (0.4-ml portions added at 10-min intervals). Heating at 55°C was continued for 50 min after the addition was complete. Most of the hydrochloric acid was removed overnight by evaporation from an open dish in the hood. The thick liquid or glassy residue, consisting mainly of 1-methylalloxan-3-acetic acid (Fig. 4, compound 2) and potassium chloride, was treated with 10 ml methanol. The resulting solution was removed with a pipette from the precipitate of potassium chloride and taken to

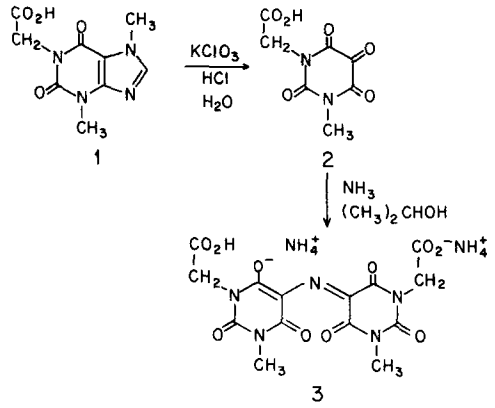

FIGURE 4. Chemical pathway for the synthesis of DMPDAA.

dryness in a rotary evaporator. To remove the remaining small amount of hydrogen chloride, methanol (20 ml) was added to the residue and removed completely by distillation under reduced pressure in a rotary evaporator; this process was carried out three times. The alloxan derivative (Fig. 4, compound 2) was then extracted from the residue into isopropyl alcohol (16 ml) and small amounts of the remaining precipitated potassium chloride were removed by centrifugation. The solution was placed in a crystallizing dish and evaporated in a vacuum desiccator to leave the product on the bottom of the dish as a thin glassy deposit. This was further freed of water and hydrogen chloride by storage in a vacuum desiccator over anhydrous magnesium sulfate and sodium hydroxide.

The crude 1-methylalloxan-3-acetic acid (Fig. 4, compound 2) thus obtained was dissolved in 15 ml of isopropyl alcohol. A small crystallizing dish (50 ml) containing this solution and a magnetic stirring bar was placed in a larger crystallizing dish of sufficient diameter to accommodate several lumps (~1 cm diameter) of ammonium carbonate (source of NH_3 for the reaction of structure 2 to structure 3 in Fig. 4) placed around the smaller dish holding the solution. A loosely fitting lid (a Petri dish) was used to cover the outer dish. The solution was stirred at room temperature while it was exposed to the enclosed ammonia atmosphere evolved by the ammonium carbonate. Stirring was continued for several hours (often over-

night) while a deep purple murexide color developed and the purple-black dye (structure 3 in Fig. 4) precipitated after the solution reached saturation. After no further accumulation of dye was evident, the solution and precipitated dye were transferred to a centrifuge tube. After centrifugation and decantation of the supernatant, the dye at the bottom of the tube was dissolved in 10 ml of methanol and precipitated by the addition of ~20 ml dry ether. After centrifugation and removal of the supernatant, a second reprecipitation of the product from 10 ml methanol with 20 ml ether was carried out in the same manner. The precipitated dye was washed in the tube with ~30 ml dry ether, centrifuged down, and dried completely by placing the tube in a vacuum desiccator after the ether had been removed by decantation. usually 0.15–0.25 g of the murexide dye was obtained by this procedure and it had a molar extinction coefficient $\epsilon(528)$ of $0.5–0.8 \times 10^4$ $M^{-1}cm^{-1}$.

At this stage, further precipitations from more dilute methanol solutions with a smaller proportion of ether could be used to secure a more purified dye. A sample of 0.21 g [$\epsilon(528) = 0.78 \times 10^4$ $M^{-1}cm^{-1}$] was dissolved in 20 ml methanol and precipitated by the addition of 25 ml dry ether. The precipitate was redissolved in 5 ml methanol, precipitated by addition of 25 ml ether, washed with ether in a centrifuge tube, and dried in a vacuum desiccator to yield 0.103 g of dark purple powder having $\epsilon(520) \approx \epsilon(528) = 1.01 \times 10^4$ $M^{-1}cm^{-1}$. This value of the molar extinction coefficient is less than $\epsilon(520)$ of tetramethylpurpurate, $1.58 \times$ $M^{-1}cm^{-1}$ (Maylie et al., 1987*a*), or of $\epsilon(520)$ of PDAA, 1.50×10^4 $M^{-1}cm^{-1}$. Since the difference may be due to impurities in the sample of DMPDAA, the value 1.58×10^4 $M^{-1}cm^{-1}$ from tetramethylpurpurate has been for the molar extinction coefficient of DMPDAA.

RESULTS

Similar results were obtained from experiments with either DMPDAA or PDAA inside cut muscle fibers. Since the purity of the sample of PDAA was probably greater than that of DMPDAA (see above), most of the figures in this article are from experiments with PDAA.

Diffusion of PDAA and DMPDAA in Cut Muscle Fibers

Fig. 5 *A* (●) shows the results of an indicator diffusion experiment carried out on a fiber mounted in a double Vaseline-gap chamber. 3.18 mM PDAA was added to the end-pool solutions and its concentration was monitored optically in the middle of the fiber in the central-pool region (page 600). The concentration of PDAA at the optical site, divided by that in the end pools, has been plotted as a function of time following indicator exposure. After ~30 min, the relative concentration exceeded unity, indicating that some of the indicator was bound or sequestered. By the end of the experiment, the concentration at the optical site was about 1.25 times that in the end pools.

Such binding or sequestration has been observed in similar experiments carried out with the Ca indicators arsenazo III, antipyrylazo III, and tetramethylpurpurate (Maylie et al., 1987*a–c*). In these experiments, diffusion data similar to those in Fig. 5 *A* were analyzed on the assumption that the binding of indicator was rapid and reversible and that the concentration of bound indicator was proportional to the concentration of free indicator. If the proportionality constant is denoted by R, the diffusion equation takes its usual mathematical form except that the diffusion constant, D, of free indicator is replaced by the apparent diffusion constant, $D/(R + 1)$

(Crank, 1956). Eqs. 6 and 8 in Maylie et al. (1987*b*) describe the time course of indicator concentration that is expected at the optical site under these assumptions for the conditions of our experiments. The continuous curve in Fig. 5 *A*, which represents a least-squares fit of these equations, provides a good fit to the experimental data. The values of the fitted parameters are $D/(R + 1) = 1.15 \times 10^{-6}$ cm^2/s and $(R + 1) = 1.27$; consequently, $D = 1.46 \times 10^{-6}$ cm^2/s. According to this analysis, the fraction of indicator inside a fiber that is freely diffusible is equal to $1/(R + 1) = 0.79$ and the fraction that is bound or sequestered is equal to $R/(R + 1) = 0.21$.

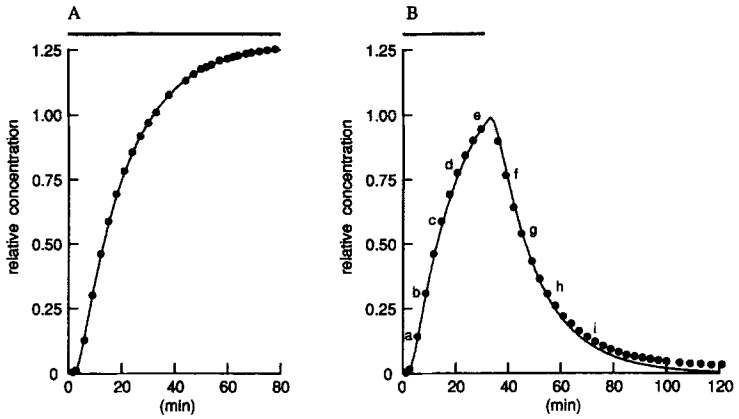

FIGURE 5. Diffusion of PDAA in cut muscle fibers. At $t = 0$, PDAA was added to the end-pool solutions where it remained for the period of time indicated by the horizontal bars. The concentration of indicator in the fiber at the optical recording site (in the middle of the central-pool region, 550 μm from the end pools [Irving et al., 1987, Fig. 1]) was estimated from measurements of indicator-related $A(520)$. This concentration, divided by that used in the end pools, is plotted as a function of time (●). The continuous curves are least-squares fits of Eqs. 6 and 8 in Maylie et al. (1987*b*); these equations assume that free indicator moves along the inside of a fiber according to the laws of one-dimensional diffusion and that the concentration of bound or sequestered indicator is directly proportional to that of free indicator. The concentrations used in the end pools were 3.18 mM in *A* (fiber 050988.1; diameter, 90–86 μm during the course of the experiment) and 5.48 mM in *B* (fiber 062888.1; diameter, 85–78 μm during the course of the experiment). The indicator was added to the end pools 29 min after saponin treatment of the end-pool segments in *A* and 28 min after treatment in *B*. In *B*, the letters *a–i* refer to traces in Fig. 11 and points in Figs. 12 and 13. The traces in Fig. 10 were taken at point *a*.

Fig. 5 *B* shows the results of an experiment that was similar to the one in Fig. 5 *A* except that PDAA remained in the end-pool solutions for only 31 min, as indicated by the horizontal bar. When the indicator was added to the end-pool solutions, its concentration at the optical site began to increase; soon after its removal, the concentration decreased. The continuous curve shows the least-squares fit of the equations for diffusion plus linear reversible binding, with $D/(R + 1) = 1.25 \times 10^{-6}$ cm^2/s, $(R + 1) = 1.19$, and $D = 1.49 \times 10^{-6}$ cm^2/s. The curve provides a good fit to the data, except possibly at late times, after the point marked *h*, when the concen-

tration points were consistently above the theoretical curve. The poor fit at late times could be due to a maintained component of indicator binding or to a small amount of indicator remaining in the end-pool solutions after the rinse period at t = 31 min.

Table I *A* gives information obtained from the analysis of PDAA diffusion in seven fibers. The concentration of indicator in the end-pool solutions and the duration of exposure are given in columns *2* and *3*. The values of the fitted parameters are given in columns *4–6*. On average, $D/(R + 1) = 1.07 \times 10^{-6}$ cm^2/s (column *4*), $(R + 1) = 1.23$ (column *5*), and $D = 1.31 \times 10^{-6}$ cm^2/s (column *6*).

TABLE I

Parameters Associated with the Analysis of Indicator Diffusion in Cut Fibers

1 Fiber reference	2 Indicator concentration	3 Indicator exposure	4 $D/(R + 1)$	5 $(R + 1)$	6 D
	mM	*min*	$\times 10^{-6}$cm^2/s		$\times 10^{-6}$cm^2/s
(A) PDAA					
040688.2	2.57	76	1.07	1.18	1.26
040788.1	2.77	81	0.93	1.30	1.21
050988.1	3.18	78	1.15	1.27	1.46
052588.1	1.44	127	0.98	1.02	1.00
062388.1	4.36	36	1.16	1.37	1.59
062888.1	5.48	31	1.25	1.19	1.49
062988.1	4.95	33	0.93	1.25	1.16
Mean			1.07	1.23	1.31
SE of mean			0.05	0.04	0.08
(B) DMPDAA					
060487.1	2.25	97	0.74	1.30	0.96
061087.1	2.48	48	0.96	1.42	1.36
061587.1	1.45	96	1.21	1.51	1.82
071387.1	1.73	42	0.93	1.50	1.39
071487.1	1.41	43	1.04	1.37	1.42
100787.1	5.16	38	1.36	1.44	1.95
100987.1	2.70	34	1.10	1.32	1.45
101687.1	2.35	63	1.05	1.29	1.35
102287.1	2.03	68	1.18	1.32	1.56
102887.1	1.84	42	1.23	1.27	1.56
Mean			1.08	1.37	1.48
SE of mean			0.06	0.03	0.09

A and *B* give results obtained from experiments with PDAA and DMPDAA, respectively. Column *1* gives the fiber reference; column *2* gives the concentration of indicator used in the end-pool solutions; column *3* gives the period of time that indicator was present in the end-pool solutions. Columns *4* and *5* give $D/(R + 1)$ and $(R + 1)$, respectively, obtained from fits of Eqs. 6 and 8 in Maylie et al. (1987*b*) to the time course of indicator concentration at the optical recording site; column *6* gives the product of columns *4* and *5*. In *A*, indicator was added to the end pools 25–46 min (average value, 33 min) after saponin treatment. In *B*, indicator was added to the end pools 35–64 min (average value, 46 min) after saponin treatment.

Table I *B* gives information from 10 fibers that were studied with DMPDAA. On average, $D/(R + 1) = 1.08 \times 10^{-6}$ cm^2/s, $(R + 1) = 1.37$, and $D = 1.48 \times 10^{-6}$ cm^2/s. The average values of $D/(R + 1)$ and D are not significantly different (see page 600) from those obtained with PDAA. The average value of $(R + 1)$ is the same

as that obtained with tetramethylpurpurate (Maylie et al., 1987*a*) and both averages of $(R + 1)$ are significantly different from that obtained with PDAA. Thus, PDAA appears to be bound or sequestered inside a muscle fiber to a lesser extent than either DMPDAA or tetramethylpurpurate.

The average values of D for PDAA and DMPDAA are slightly smaller than that obtained under similar conditions for tetramethylpurpurate, 1.75×10^{-6} cm^2/s (although the difference is statistically significant only for PDAA). This is expected since PDAA and DMPDAA are somewhat larger molecules (molecular weights, 380 and 408, respectively) than tetramethylpurpurate (molecular weight, 322) and their diffusion constants were measured at a slightly lower temperature (16°C compared with 18°C). In skinned muscle fibers studied at 20°C, the (longitudinal) diffusion constants of sucrose (molecular weight, 342) and ATP (molecular weight, 507) are 2.1×10^{-6} cm^2/s and 1.2×10^{-6} cm^2/s, respectively (Kushmerick and Podolsky, 1969). The average values of D for PDAA and DMPDAA diffusion in cut fibers, 1.31×10^{-6} cm^2/s and 1.48×10^{-6} cm^2/s, respectively, are within this range and consequently are similar to those expected for compounds of their size diffusing longitudinally in a skinned muscle fiber.

Wavelength Dependence of the Absorbance of PDAA and DMPDAA Inside Resting Fibers

According to the wavelength dependence of the absorbance spectrum, 0.11–0.15 of the tetramethylpurpurate inside a resting cut muscle fiber appears to be complexed with Ca (Maylie et al., 1987*a*). This is surprising since the dissociation constant of the indicator, 2.6 mM, is 10^4–10^5 times the value of myoplasmic resting free [Ca] (Blinks et al., 1982). One of the explanations offered by Maylie et al. (1987*a*) was that some of the tetramethylpurpurate inside a fiber might enter the high free [Ca] environment of the SR and become partially complexed with Ca. Since PDAA, with two ionized acetate groups, is expected to be less permeant than tetramethylpurpurate, it was of interest to determine the fraction of PDAA that appears to be complexed with Ca inside a resting cut fiber.

Fig. 6 (●) shows the PDAA-related absorbance, $A(\lambda)$, normalized by $A(520)$ and plotted as a function of wavelength, λ. The continuous curve, which is the normalized [Ca] = 0 mM cuvette spectrum from Fig. 2 *A*, provides a good fit to the experimental points. A similar good fit to resting abosrbance spectra was obtained in two other fibers.

Although the [Ca] = 0 mM cuvette spectrum provides a good fit to the wavelength dependence of PDAA absorbance in a resting fiber, it seemed desirable to have a quantitative way to estimate the fraction of indicator that appears to be complexed with Ca. To do this, the data in Fig. 6 were least-squares fitted by a linear combination of the normalized Ca-free and normalized Ca-complexed spectra (not shown), constrained so that the sum of the two scaling factors was equal to unity. The fraction of indicator that appears to be complexed with Ca, f, is given by the scaling factor for the contribution of the Ca-complexed spectrum to the fit. If all the indicator was Ca-free, f should be zero or, because of noise in the data, a small positive or negative number. A best least-squares fit to the data in Fig. 6 gave $f = -0.0052$ (3.05–3.35 mM PDAA). In two other fibers, $f = -0.0124$ (3.21–3.74 mM

PDAA) and −0.0145 (1.40–1.44 mM PDAA). The average value from the three fibers, −0.0107, is not significantly different from zero.

Resting absorbance spectra were also measured in six fibers that contained 1.53–3.00 mM DMPDAA. The average value of f, 0.0112 (SEM = 0.0057), is also not significantly different from zero.

The conclusion of this section is that the absorbance spectra of PDAA and DMPDAA inside resting muscle fibers match the corresponding [Ca] = 0 mM cuvette spectra. This finding, which stands in contrast to that obtained with tetra-

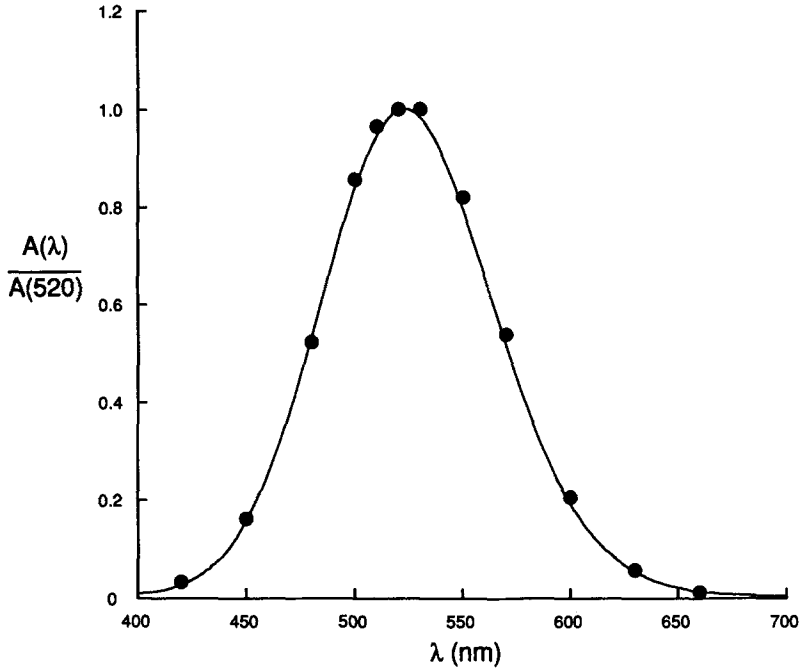

FIGURE 6. Absorbance spectrum of PDAA inside a resting muscle fiber. The circles show indicator-related $A(\lambda)$, normalized by the value at 520 nm, plotted as a function of wavelength. The measurements were made 46–71 min after indicator was added to the end-pool solutions or 92–117 min after saponin treatment of the end-pool segments. The concentration of indicator at the optical site was 3.05–3.35 mM; the diameter of the fiber was 88 μm. Fiber 040788.1. The curve shows the normalized [Ca] = 0 mM absorbance spectrum from Fig. 2 *A*.

methylpurpurate, is consistent with the idea that PDAA and DMPDAA exist in a Ca-free state inside resting muscle fibers, presumably because their acetate groups prevent entry into the high free [Ca] environment of the SR. Although this explanation seems likely, we cannot rule out the possibility that some of the indicator inside a resting fiber is complexed with Ca, and that the expected blue shift in its absorbance spectrum (Fig. 2 *A*) is masked by a red shift in the spectrum that might occur when the indicator is introduced into a muscle fiber, similar to the red shift that is observed when antipyrylazo III is introduced into either intact fibers (Baylor et al.,

1986) or cut fibers (Maylie et al., 1987*c*). For example, if 2.5% of the PDAA inside a fiber were complexed with Ca, a 2-nm red-shift in the absorbance spectra of both Ca-free and Ca-complexed indicator would produce a resting absorbance spectrum that resembles the [Ca] = 0 mM curve in Fig. 6 (although its half-width would be 1.7 nm greater).

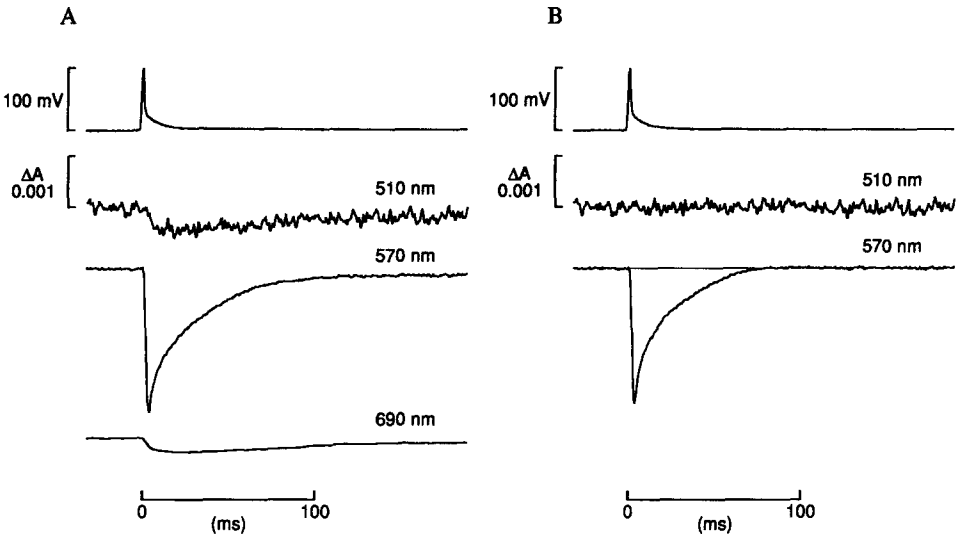

FIGURE 7. Changes in absorbance, after action potential stimulation, of a fiber containing 3.27 mM PDAA. (*A*) The top trace shows the action potential and the next three traces show changes in absorbance measured simultaneously at three different wavelengths, as indicated. The signals were filtered by 0.625-kHz eight-pole Bessel filters that attenuated and slightly modified the shape of the electrical signal but did not attenuate the optical signals (Irving et al., 1987, Fig. 16); the actual peak amplitude of the action potential, measured on a storage oscilloscope, was 135 mV. The 690-nm signal was additionally filtered by a 0.1 kHz Gaussian digital filter (Colquhoun and Sigworth, 1983). The records were taken 61 min after indicator was added to the end pools or 107 min after saponin treatment of the end-pool segments. The contribution made by the intrinsic signal to the absorbance changes at 510 and 570 nm was estimated as described in the text. (*B*) The top trace shows the action potential from *A*. The next two traces show the changes in indicator-related absorbance at 510 and 570 nm, obtained from the corresponding traces in *A* by subtraction of the estimated intrinsic signal (given by the 690-nm trace scaled by $[\lambda/690]^{-1.46}$). In this and the following figures, the vertical tick at $t = 0$ on the time axis corresponds to the moment that the electrical stimulus was started, shifted 1.6 ms to the right to allow for the low frequency delay of the 0.625 kHz eight-pole Bessel filters. From the experiment illustrated in Fig. 6.

Changes in Absorbance after Action Potential Stimulation of a Fiber Containing PDAA

Fig. 7 *A* shows an action potential (top trace) and three traces of changes in fiber absorbance, $\Delta A(\lambda)$, simultaneously recorded at the indicated wavelengths. The optical traces contain different amounts of noise. The $\Delta A(510)$ trace contains more

noise than the $\Delta A(570)$ and $\Delta A(690)$ traces for two main reasons: it was recorded with a 10-nm, rather than a 30-nm, bandpass interference filter and the optical apparatus is less sensitive to 510-nm light than to 570- and 690- nm light. The $\Delta A(690)$ trace is less noisy than the $\Delta A(570)$ trace, mainly because it has been additionally filtered by a 0.1 kHz Gaussian digital filter (Colquhoun and Sigworth, 1983); this filter does not distort the time course of the signal (Irving et al., 1987, Fig. 16 *B*).

Since PDAA, either Ca-free or Ca-complexed, does not appreciably absorb 690-nm light, the $\Delta A(690)$ trace in Fig. 7 *A* shows the intrinsic absorbance change of the fiber at 690 nm. The $\Delta A(510)$ and $\Delta A(570)$ traces also contain intrinsic components and, in addition, may contain components due to an absorbance change of the indicator.

The intrinsic components of the $\Delta A(510)$ and $\Delta A(570)$ traces in Fig. 7 *A* were estimated with the procedure used with tetramethylpurpurate (Maylie et al., 1987*a*). The $\Delta A(510)$ trace was least-squares fitted by a linear combination of the $\Delta A(690)$ and $\Delta A(570)$ traces. The scaling factors, 1.551 for the 690-nm trace and 0.003 for the 570-nm trace, were used to determine the wavelength dependence of the intrinsic signal on the following assumptions: (*a*) that the intrinsic signal has the same waveform at 510, 570, and 690 nm and has an amplitude that varies with wavelength according to λ^{-n} (Baylor et al., 1982*a*; Irving et al., 1987), (*b*) that the $\Delta A(690)$ signal is purely intrinsic whereas the $\Delta A(570)$ and $\Delta A(510)$ signals each contains an intrinsic component plus, possibly, an indicator-related component, and (*c*) that the indicator-related components at 510 and 570 nm have the same waveform but, in general, different amplitudes. The scaling factors 1.551 and 0.003 give a value of 1.46 for n, which can then be used to scale the $\Delta A(690)$ intrinsic signal by $(\lambda/690\text{ nm})^{-n}$ to give the intrinsic contributions at different wavelengths.

The top trace in Fig. 7 *B* shows the action potential from Fig. 7 *A*. The next two traces show the indicator-related $\Delta A(510)$ and $\Delta A(570)$ signals, obtained from the corresponding traces in Fig. 7 *A* by subtraction of the $\Delta A(690)$ trace scaled by $(\lambda/690\text{ nm})^{-1.46}$. The $\Delta A(510)$ trace is flat, as expected since 510 nm is near the isosbestic wavelength of PDAA, which was estimated in cuvette calibrations to be 511 nm (see pages 601–602 and Fig. 2). The $\Delta A(570)$ trace shows an early decrease in indicator-related absorbance that rapidly returned to the prestimulus baseline, which is indicated by the thin horizontal line.

Wavelength Dependence of Changes in PDAA and DMPDAA Absorbance after an Action Potential

Fig. 8 *A* shows changes in PDAA-related absorbance, at the indicated wavelengths, in a fiber that was stimulated at $t = 0$ to give a single action potential. The $\Delta A(450)$ and $\Delta A(480)$ traces show an early, transient increase in absorbance whereas the $\Delta A(550)$ and $\Delta A(570)$ traces show an early, transient decrease. The $\Delta A(510)$ and $\Delta A(660)$ traces are essentially flat.

Fig. 8 *B* shows the same $\Delta A(\lambda)$ traces as Fig. 8 *A* . The simultaneously recorded $\Delta A(570)$ signal, scaled to least-squares fit each $\Delta A(\lambda)$ signal, is shown superimposed on each $\Delta A(\lambda)$ trace. Within the error of the measurements, the scaled $\Delta A(570)$ signals provide good fits to the $\Delta A(\lambda)$ signals, which is consistent with the idea that

only one kind of change in PDAA absorbance occurred during the first 100 ms following an action potential.

Fig. 9 shows the wavelength dependence of this absorbance change. The filled circles are the scaling factors obtained from the experiment in Fig. 8 *B*, normalized to unity at $\lambda = 570$ nm. The wavelength dependence of the circles is similar to that of the continuous curve, the normalized 10.0 mM Ca-difference spectrum from Fig. 2 *B*, except at 420 and 450 nm where the $\Delta A(\lambda)$ traces were very noisy (Fig. 8). Similar good agreement was found in two other experiments on fibers containing PDAA and in five experiments on fibers containing DMPDAA. This provides strong evidence that the transient changes in PDAA and DMPDAA absorbance, such as

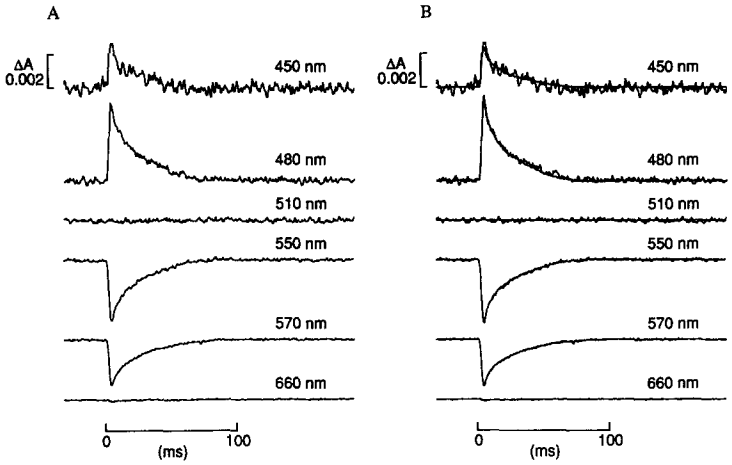

FIGURE 8. Wavelength dependence of the $\Delta A(\lambda)$ signal elicited by action potential stimulation. (*A*) Traces of indicator-related absorbance at six different wavelengths. All signals, including that at 570 nm, were recorded with 10-nm bandpass interference filters in the λ_1 position (Irving et al., 1987, Fig. 2). (*B*) Same absorbance traces as in *A*. Each λ_1 trace was least-squares fitted by scaling the simultaneously recorded $\Delta A(570)$ trace, taken with a 30-nm bandpass filter in the λ_2 position (Irving et al., 1987, Fig. 2) and corrected for the intrinsic contribution; the scaled $\Delta A(570)$ traces are shown superimposed. Additional information is given in the legends of Figs. 6 and 7.

those shown in Figs. 7 and 8, are due to Ca complexation by the indicator. Hereafter, the indicator-related $\Delta A(570)$ signal will sometimes be called the Ca signal.

Although the signal-to-noise ratio of the Ca signal recorded from cut fibers containing either PDAA (Figs. 7 *B* and 8), DMPDAA (Fig. 14, below), or tetramethylpurpurate (Maylie et al., 1987*a*) allows adequate resolution of the main features of the signal, the ratio is not as large as that recorded under similar conditions with arsenazo III or antipyrylazo III (Maylie et al., 1987*b*, *c*). If the concentration of each indicator is adjusted so that the same concentration of Ca is complexed at the time of the peak of the Ca signal, the optical signal from arsenazo III or antipyrylazo III would have a larger signal-to-noise ratio than that from PDAA, DMPDAA, or tetra-

methylpurpurate. One reason for this difference is that, when Ca is complexed, the peak change in molar extinction coefficient is larger with arsenazo III and antipyrylazo III than with the purpurate indicators. At the wavelengths usually used for measuring Ca signals, the changes in $\Delta\epsilon(\lambda)$ (referred to the complexation of one Ca) are about 2–3 $\times$ 10^4 $M^{-1}cm^{-1}$ with arsenazo III and antipyrylazo III (Rios and Schneider, 1981; Palade and Vergara, 1983; Hollingworth et al., 1987) but only 0.7–0.9 $\times$ 10^4 $M^{-1}cm^{-1}$ with the purpurate indicators (Methods sections in this article and in Maylie et al., 1987*a*). Another reason that the signal-to-noise ratio is larger with arsenazo III and antipyrylazo III than with the purpurate indicators is that the peak change in $\Delta\epsilon(\lambda)$ for arsenazo III and antipyrylazo III occurs at longer wavelengths, where the sensitivity of our optical apparatus is greater, owing to a greater light intensity from the tungsten-halogen bulb and to a greater quantum efficiency of the photodiodes.

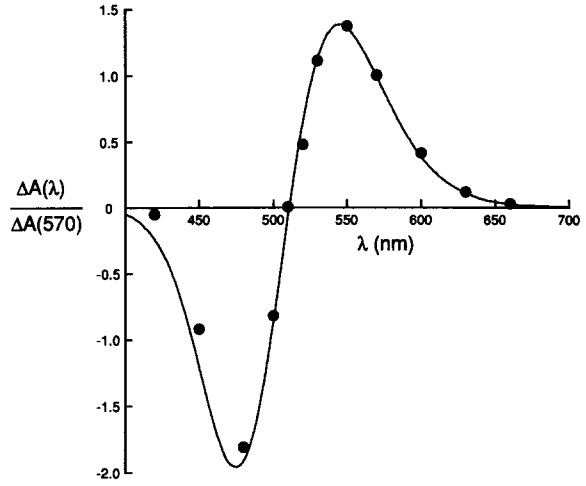

FIGURE 9. Wavelength dependence of the amplitude of the $\Delta A(\lambda)$ signal elicited by action potential stimulation, from the experiment illustrated in Fig. 8 *B*. The scaling factors used to fit the $\Delta A(570)$, λ_2 signals to the $\Delta A(\lambda)$, λ_1 signals are plotted as a function of λ; they have been normalized by the value at 570 nm. The curve shows the normalized 10.0 mM Ca-difference spectrum from Fig. 2 *B*.

Correction of $\Delta A(570)$ Signals for Changes in Indicator Concentration during the Sampling Period

Soon after an indicator is either added to or removed from the end-pool solutions, the rate of change of indicator concentration at the optical recording site can be sufficiently large that a noticeable slope is added to the $\Delta A(\lambda)$ signals at wavelengths absorbed by the indicator. This section describes the method that was used to correct Ca signals for this component. This correction was not required for Figs. 7–9, since the concentration of indicator at the optical site changed little during the period when the measurements were made.

Fig. 10 *A* shows traces that were taken 5.5 min after 5.48 mM PDAA had been added to the end-pool solutions (Fig. 5 *B*, point *a*). The top trace shows an action potential and the next two traces show the associated $\Delta A(570)$ and $\Delta A(690)$ signals. The bottom trace shows the $\Delta A(570)$ signal after its intrinsic component, which was estimated according to the method illustrated in Fig. 7 *B*, had been subtracted.

After 50–100 ms, when the transient Ca signal was over, the $\Delta A(570)$ trace continued to increase slowly above the level of its prestimulus baseline, indicated by a thin horizontal line.

During the period in Fig. 10 *A* that data were sampled, PDAA was diffusing into the optical recording site, thereby increasing the fiber's absorbance at 570 nm. The rate of change of both the concentration of PDAA and its absorbance at 570 nm

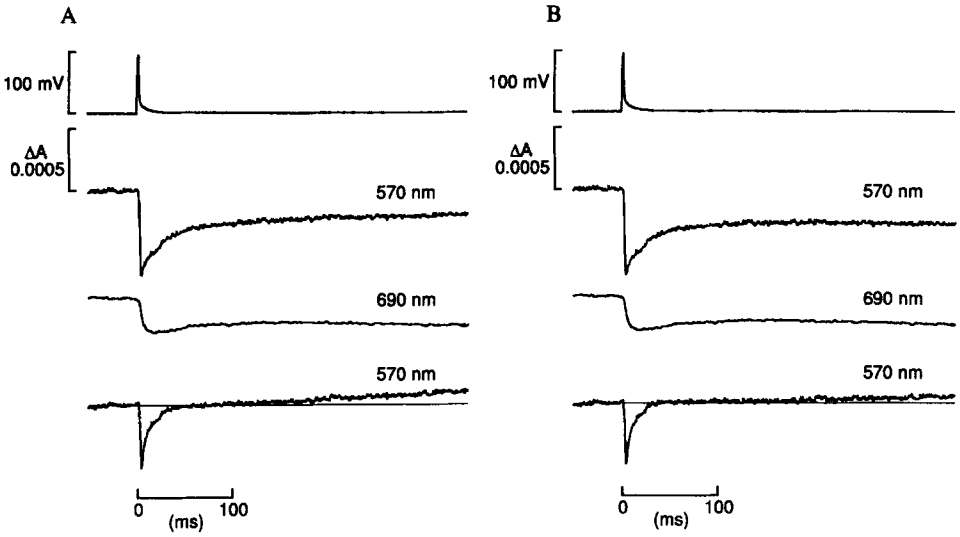

FIGURE 10. Correction of the $\Delta A(570)$ trace for the increase in absorbance associated with indicator diffusing into the optical recording site during the sampling period. (*A*) The top trace shows the action potential (actual amplitude, 130 mV) and the next two traces show the changes in fiber absorbance recorded simultaneously at 570 and 690 nm. The bottom trace shows the 570-nm trace corrected for the intrinsic contribution as illustrated in Fig. 7; for this correction, the 690-nm trace was scaled by $(570/690)^{-1.45}$ and subtracted from the 570-nm trace. A horizontal line has been drawn through the prestimulus baseline. *B* has the same format as *A*. The action potential and 690-nm trace are the same as those in *A*. The upper 570-nm trace was obtained from the corresponding trace in *A*; a small positive slope, determined from the slope of the theoretical curve at point a in Fig. 5 *B*, was subtracted from the trace in *A* to correct for the increase in absorbance associated with the increase in indicator concentration at the optical recording site during the sampling period. The bottom trace shows the indicator-related change in 570-nm absorbance, which was obtained by subtraction of the 690-nm trace scaled by $(570/690)^{-1.99}$. From the experiment illustrated in Fig. 5 *B*, point *a*; the concentration of indicator at the optical site was 0.77 mM; the fiber diameter was 85 μm.

were estimated from the slope of the theoretical curve at point *a* in Fig. 5 *B*. Fig. 10 *B* shows the action potential and the $\Delta A(690)$ signal from Fig. 10 *A*. The upper 570-nm trace in Fig. 10 *B* was obtained from the corresponding trace in Fig. 10 *A*, after correction for the small progressive increase in absorbance that was associated with the diffusion of indicator into the optical site. The bottom 570-nm trace shows the indicator-related $\Delta A(570)$ signal, with the prestimulus baseline superimposed.

The trace has a small, positive slope at late times but its magnitude is only one-third that in Fig. 10 *A*. Thus, the correction removes most, but in some cases not all, of the changes in absorbance that are associated with changes in indicator concentration during the sampling period. This method of correction was used in Figs. 11–16 and in Table II.

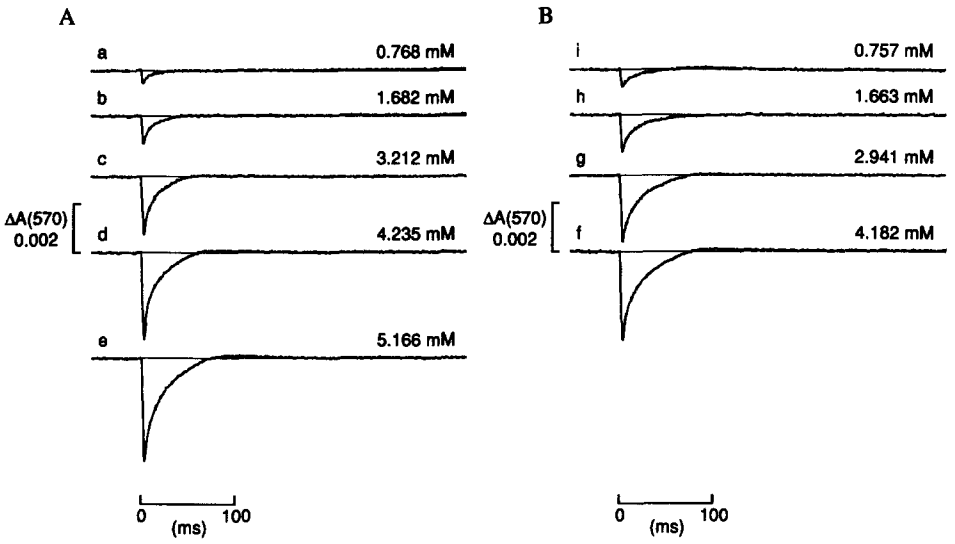

FIGURE 11. Effect of indicator concentration on the indicator-related $\Delta A(570)$ signal that is elicited by action potential stimulation in a fiber containing PDAA, from the experiment illustrated in Figs. 5 *B* and 10. The traces in *A* were obtained while the indicator was present in the end-pool solutions; those in *B* were obtained after its removal. The concentration of indicator is indicated beside each trace. The $\Delta A(570)$ traces were corrected, as illustrated in Fig. 10, for the changes in indicator-related absorbance associated with indicator diffusing into (*A*) or out of (*B*) the optical recording site during the sampling period. The chronological order of the measurements is from *a* to *i*(see Fig. 5 *B*). During this period, the diameter of the fiber decreased from 85 to 82 μm, the amplitude of the action potential decreased from 130 to 127 mV, and the holding current changed from −43 to −39 nA. The linear cable parameters, r_m, r_i, and r_e were estimated as described in Irving et al. (1987); r_m is the external membrane resistance of a unit length of fiber, r_i is the internal longitudinal resistance per unit length, and r_e is the external resistance under the Vaseline seals per unit length. From *a* to *i*, the estimate of r_m decreased from 0.109 to 0.085 MΩ·cm, that of r_i decreased from 5.04 to 4.94 MΩ/cm, and that of $r_e/(r_e + r_i)$ increased from 0.969 to 0.973.

Effect of Indicator Concentration of the Ca Signal Recorded with PDAA

Fig. 11 shows Ca signals recorded with different concentrations of PDAA inside a cut muscle fiber. The signals have been corrected, as described in the preceding section, for changes in 570-nm absorbance associated with changes in indicator concentration during the sampling period. *A* shows indicator-related $\Delta A(570)$ signals taken during the period when indicator was present in the end-pool solutions and was diffusing into the optical site (Fig. 5 *B*). The traces are plotted in chronological

order, from *a* to *e*, with the concentration of indicator written beside each record. As the indicator concentration increased, the amplitude of the Ca signal increased. Fig. 11 *B* shows $\Delta A(570)$ traces taken after indicator had been removed from the end-pool solutions. In chronological order, from *f* to *i*, the concentration of indicator decreased and the amplitude of the Ca signal decreased. Throughout the experimental period, from *a* to *i*, the electrical condition of the fiber remained stable (information given in legend of Fig. 11).

During the period 75–150 ms after stimulation, traces *e* and *f* in Fig. 11 are slightly above the prestimulus baseline. Small positive components are also present in traces *d*, *g*, and *i*. The amplitude of such components varied from fiber to fiber

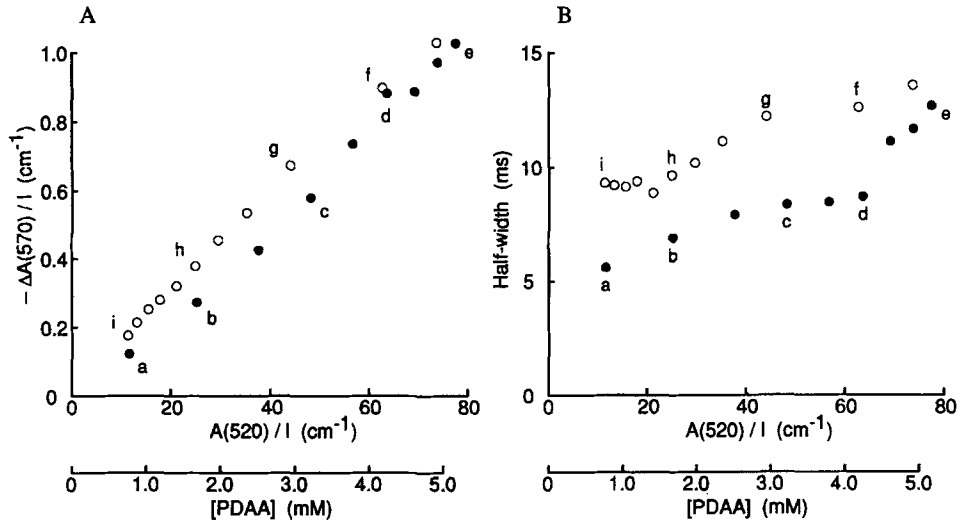

FIGURE 12. Effect of PDAA concentration on the peak amplitude (*A*) and half-width (*B*) of the indicator-related $\Delta A(570)$ signal elicited by action potential stimulation, from the traces in Fig. 11 and others taken during the same experiment. The values of $A(520)$ and $\Delta A(570)$ have been divided by the optical path length, *l*, to allow for the small change in fiber diameter, from 85 to 82 μm, that took place during the experiment. There are two horizontal axes, one marked in units of $A(520)/l$ and the other in units of indicator concentration. The filled circles are from traces taken during the period when indicator was present in the end-pool solutions; the open circles are from traces taken after its removal. In *A*, the value of $\Delta A(570)/l$ at point *e* corresponds to 109 μM [Ca] being complexed by the indicator.

and, in a particular fiber, sometimes changed during the time course of an experiment. In Fig. 11, for example, the amplitude was larger in traces *i* and *f* than in *a* and *d*. In one fiber (not illustrated), the 570-nm traces had relatively large positive components, with amplitudes 0.2–0.3 times those of the early negative-going signal. A positive component was also present on the trace at 510 nm, near the isosbestic wavelength, suggesting that this component is not related to a change in Ca complexation by the indicator, but is probably due to movement or some other artifact.

Figs. 12 and 13 show some of the properties of the Ca signals, from the experi-

ment illustrated in Fig. 11, plotted as a function of $A(520)/l$ or PDAA concentration. Filled circles refer to values obtained during the period when indicator was present in the end pools and open circles refer to values obtained after its removal.

Fig. 12 *A* shows a plot of the peak amplitude of the PDAA-related $\Delta A(570)/l$ signal. The amplitude of peak free [Ca] appeared to increase somewhat during the experiment, as indicated by the gentle upward and downward curvatures of the relations described by the filled and open circles, respectively; as a result, the open circles lie above the filled circles. A similar progressive increase in peak free [Ca] was found in four out of eight experiments. Nonetheless, the relation between peak $\Delta A(570)/l$ and indicator concentration was approximately linear in all experiments (cf. Fig. 12 *A*), as expected if peak free Δ[Ca] remained constant during the experiment and if PDAA forms predominantly 1:1 complexes with Ca (see Methods).

In Fig. 12 *A*, the peak fraction of indicator, f, that was complexed with Ca varied from a minimum of 0.0165 at point *a* to a maximum of 0.0256 between points *h* and *i*; these values were estimated from the values of indicator-related $\Delta A(570)/l$ and $A(520)/l$ as described in Methods. If all the PDAA was able to react with Ca as it does in cuvette calibrations, the average value of f over the concentration range 2.0–5.2 mM corresponds to 20.8 μM peak free [Ca] (Eq. 2). If only freely diffusible PDAA—equal to the total concentration of indicator divided by $(R + 1)$ (Table I *A*, column 5)—could so react, peak free [Ca] was 24.7 μM.

Values of peak free [Ca] after an action potential were estimated in six fibers containing 2.0–5.2 mM PDAA. The overall average was 20.7 μM (SEM, 1.0 μM), on the assumption that all the indicator was able to react normally with Ca, and 26.2 μM (SEM, 1.7 μM), on the assumption that only freely diffusible indicator could so react.

Fig. 12 *B* shows a plot of the half-width of the indicator-related $\Delta A(570)$ signal. During the period when the indicator was present in the end-pool solutions (●), the half-width increased from 5.6 ms at point *a* to 12.7 ms at point *e*. After the indicator was removed (○), the half-width decreased and was 9.3 ms at point *i*. Since the concentration of indicator was approximately the same when measurements *a* and *i* were made, the increase in half-width from 5.6 to 9.3 ms most likely reflects a change in the condition of the fiber that occurred during the 65-min period that elapsed between the two measurements. An increase in half-width was also consistently observed in experiments with arsenazo III (Maylie et al., 1987*b*) and antipyrylazo III (Maylie et al., 1987*c*) and, similar to the experiment in Fig. 12 *B*, was not associated with any deterioration in the electrical condition of the fiber. It may be due to changes in the composition of the myoplasmic solution at the optical recording site brought about by diffusional equilibration with the end-pool solutions (Maylie et al., 1987*c*).

In Fig. 12 *B*, the increase in half-width from *a* to *e* and the decrease from *e* to *i* suggest that an increase in indicator concentration in itself may increase the half-width of the Ca signal in a direct and reversible manner. This could be related to the Ca buffering capacity of the indicator or perhaps to some reversible pharmacological action.

Fig. 13 shows a plot of the ratio of PDAA-related $\Delta A(570)_{steady}/\Delta A(570)_{peak}$, in

which $\Delta A(570)_{steady}$ is taken as the average value of $\Delta A(570)$ measured 200–350 ms after stimulation. Since PDAA is a low affinity Ca indicator, $\Delta A(570)_{steady}/\Delta A(570)_{peak}$ is expected to be approximately equal to $\Delta[Ca]_{steady}/\Delta[Ca]_{peak}$. From *a* to *c*, the value of the ratio increased from −0.082 to −0.008. Thereafter, it remained reasonably constant until the increase just before the point marked *i*. The determination of the value of indicator-related $\Delta A(570)_{steady}$ depends on subtracting any $\Delta A(570)$ component that is associated with a change in indicator concentration during the sampling period (Fig. 10). It also depends on subtracting the intrinsic component from the recorded $\Delta A(570)$ signal. If the estimate of either component is in error, the value of indicator related $\Delta A(570)_{steady}$ would also be in error. Since the intrinsic correction becomes relatively smaller as the concentration of indicator is increased, its contribution to the error should also become relatively smaller. It therefore seems likely that the most accurate estimate of $\Delta A(570)_{steady}/\Delta A(570)_{peak}$ is

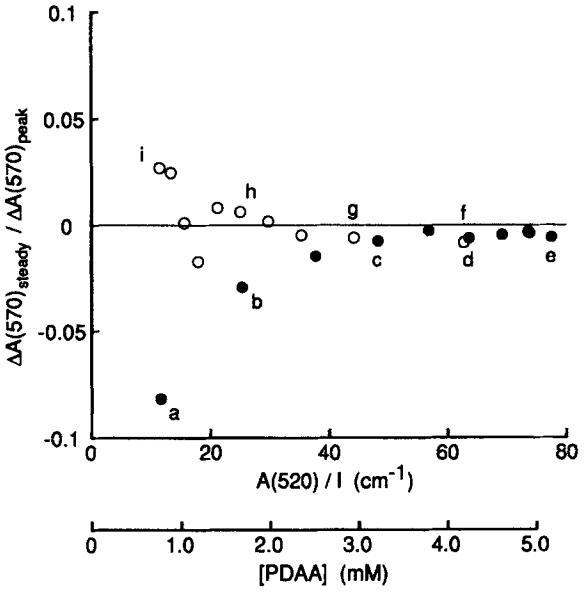

FIGURE 13. Effect of PDAA concentration on the ratio $\Delta A(570)_{steady}/\Delta A(570)_{peak}$ elicited by action potential stimulation. Same experiment and format as used in Fig. 12. $\Delta A(570)_{steady}$ represents the average value of indicator-related $\Delta A(570)$ measured 200–350 ms after stimulation.

obtained with large concentrations of indicator. For the fiber in Fig. 13, the average value of measurements made with 2.0–5.2 mM indicator was −0.0062.

Values of indicator-related $\Delta A(570)_{steady}/\Delta A(570)_{peak}$ after a single action potential were determined in six fibers containing 2.0–5.2 mM PDAA. The overall average was −0.0068 (SEM, 0.0040). This value is not significantly different from zero but is significantly different from 0.01 and 0.02, the limits of the range 0.01–0.02 estimated in intact fibers for $\Delta[Ca]_{steady}/\Delta[Ca]_{peak}$ (Hollingworth and Baylor, 1986; Baylor and Hollingworth, 1988).

Effect of Indicator Concentration on the Ca Signal Recorded with DMPDAA

Fig. 14 shows Ca signals recorded during an experiment similar to that shown in Fig. 11 except that DMPDAA, rather than PDAA, was used to measure Ca. In *A*, the

amplitude of the indicator-related $\Delta A(570)$ signal increased as the concentration of indicator at the optical site increased and, in *B*, it decreased as the indicator concentration decreased. The electrical condition of the fiber remained stable throughout the experiment (see legend of Fig. 14), as was the case in the experiment in Fig. 11.

Figs. 15 and 16 are similar to Figs. 12 and 13, respectively. Fig. 15 *A* shows the peak amplitude of the DMPDAA-related $\Delta A(570)/l$ signal plotted as a function of $A(520)/l$ or indicator concentration. The relation between $\Delta A(570)/l$ and indicator concentration is approximately linear and reversible, consistent with the idea that the active increase in myoplasmic free [Ca] remained constant during the experi-

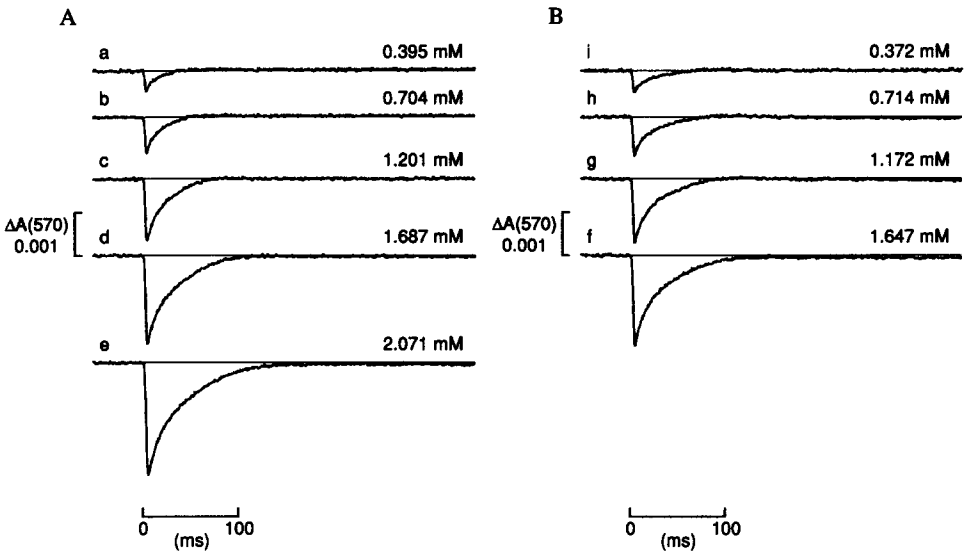

FIGURE 14. Effect of indicator concentration on the indicator-related $\Delta A(570)$ signal elicited by action potential stimulation of a fiber containing DMPDAA. Same format as Fig. 11. DMPDAA was added to the end-pool solution 46 min after saponin treatment of the end-pool segments of the fiber; it was removed 42 min later. From *a* to *i*, the diameter of the fiber decreased from 78 to 76 μm, the amplitude of the action potential decreased from 131 to 126 mV, the holding current changed from -39 to -46 nA, the estimate of r_m decreased from 0.123 to 0.081 MΩ·cm, that of r_i decreased from 4.52 to 4.23 MΩ/cm, and that of $r_e/(r_e + r_i)$ decreased from 0.974 to 0.973. Fiber 102887.1.

ment and that the predominant stoichiometry of Ca:indicator complexation is 1:1 (see Methods). None of the DMPDAA experiments showed the slight increase in peak free [Ca] during the course of the experiment that was observed in four out of eight experiments with PDAA (e.g., Fig. 12 *A*).

In the experiment in Fig. 15 *A*, peak free [Ca] was estimated from the values of indicator-related $\Delta A(570)/l$ and $A(520)/l$, as described in Methods. With 1.75–2.25 mM DMPDAA, the average value was 21.3 μM (which corresponds to 0.0265 of the indicator being complexed with Ca, Eq. 2), if all the indicator was able to react with

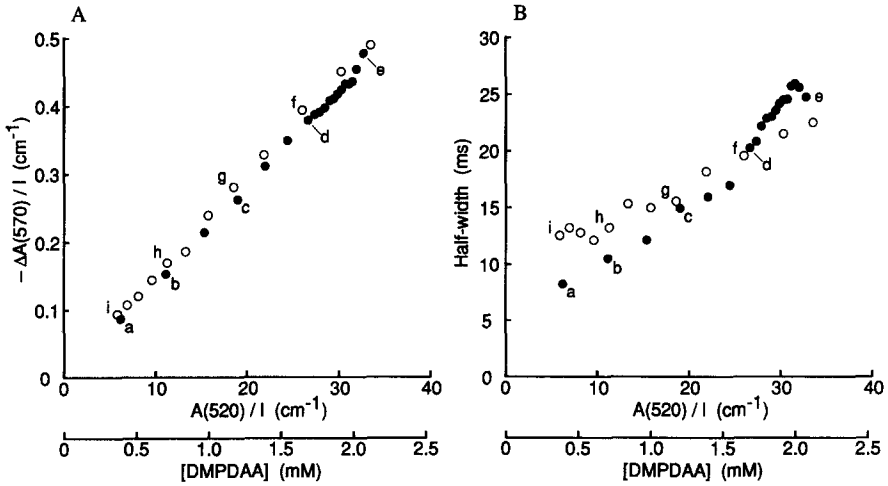

FIGURE 15. Effect of DMPDAA concentration on the peak amplitude (A) and half-width (B) of the indicator-related $\Delta A(570)$ signal elicited by action potential stimulation, from the experiment in Fig. 14. Same format as Fig. 12. In A, the value of $\Delta A(570)/l$ at point e corresponds to 57 μM [Ca] being complexed by the indicator.

Ca as it does in cuvette calibrations, and 27.0 μM, if only freely diffusible indicator could so react. Average values of peak free [Ca] from eight fibers containing 1.75–2.25 mM DMPDAA were 20.5 μM (SEM, 0.9 μM), if all the indicator was able to react with Ca, and 27.5 μM (SEM, 2.7 μM), if only freely diffusible indicator was able to so react. These values of peak free [Ca] after a single action potential are not

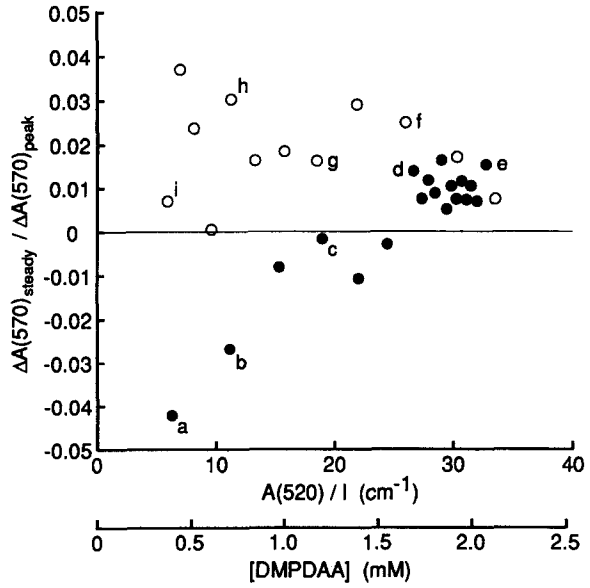

FIGURE 16. Effect of DMPDAA concentration on the ratio $\Delta A(570)_{steady}/\Delta A(570)_{peak}$ elicited by action potential stimulation, from the experiment in Fig. 14. Same format as Fig. 13.

significantly different from the corresponding average values obtained with PDAA.

Fig. 15 *B* shows a plot of the half-width of the indicator-related $\Delta A(570)$ signal. As DMPDAA entered the optical recording site, after its addition to the end pools, the half-width increased from 8.2 ms at point *a* to 24.7 ms at point *e*. After the indicator was removed from the end-pool solutions and began to diffuse out of the optical site, the half-width of the Ca signal progressively decreased and, at point *i*, was 12.5 ms.

In Fig. 15 *B*, the relation between the half-width of the Ca signal and indicator concentration had a large reversible component (from 8.2 to 12. 5 ms with 0.4 mM DMPDAA to 24.7 ms with 2.1 mM DMPDAA) that was not observed with PDAA (Fig. 12 *B*). This difference between the results with DMPDAA and PDAA cannot be explained by a difference in the Ca-buffering capacities of the indicators, since PDAA and DMPDAA have similar K_D's. The most likely explanation is that either DMPDAA itself or an impurity associated with its synthesis can increase the half-width of the Ca signal in a reversible fashion.

Fig. 16 shows a plot of the ratio of DMPDAA-related $\Delta A(570)_{steady}/\Delta A(570)_{peak}$. After the initial increase from *a* to *c*, the ratio varied between -0.01 and 0.04; with 1.75–2.25 mM indicator, the average value was 0.010. In nine fibers containing 1.75–2.25 DMPDAA, the overall average of $\Delta A(570)_{steady}/\Delta A(570)_{peak}$ was 0.0032 (SEM, 0.0085). This value is not significantly different from zero, from the average value estimated with 2.0–5.2 mM PDAA (page 618), or from either 0.01 or 0.02, the limits of the range estimated for $\Delta[Ca]_{steady}/\Delta[Ca]_{peak}$ in intact fibers (Hollingworth and Baylor, 1986; Baylor and Hollingworth, 1988).

Since an increase in the concentration of DPMDAA can markedly increase the half-width of the Ca signal (Fig. 15 *B*), the concentration of DMPDAA at the optical recording site was usually limited to $\leq$3 mM. Consequently, the average values of peak free [Ca] and $\Delta A(570)_{steady}/\Delta A(570)_{peak}$ obtained with DMPDAA were made with 1.75–2.25 mM indicator rather than with 2.0–5.2 mM indicator as was used for PDAA.

Ca Signals Recorded with Small Concentrations of PDAA and DMPDAA

Table II gives information about Ca signals that were recorded early in experiments on fibers that contained 0.5–1.0 mM PDAA or 0.4–0.6 mM DMPDAA. This concentration range allows a reliable measurement of the Ca signal with little effect on its half-width (Figs. 12 *B* and 15 *B*). Column *2* gives the concentration of indicator that was present at the optical site when the Ca signal was measured. Columns *3* and *4* give, respectively, the intervals of time that elapsed from saponin treatment to the measurement and from indicator addition to the end-pool solutions to the measurement.

The average time to half-peak of the Ca signals, after that of the action potential, was 2.4 ms with PDAA and 3.0 ms with DMPDAA (Table II, column *5*). These values are similar to those obtained under similar conditions with tetramethylpurpurate, 2.8 ms (Table III of Maylie et al., 1987*a*, the myoplasmic component), and with antipyrylazo III, 3.1 ms (Table IV of Maylie et al., 1987*c*).

The average value of the half-width of the Ca signal was 6.9 ms with PDAA and

TABLE II

Parameters Associated with Ca Signals Recorded with 0.5–1.0 mM PDAA or 0.4–0.6 mM DMPDAA

1	2	3	4	5	6	7	8	9
				ΔA(570)				
Fiber reference	Indicator concentration	Time after saponin	Time after indicator	Time to half-peak	Half-width	Steady to peak	Peak free [Ca]	Peak [Ca] ×(R + 1)
	mM	*min*	*min*	*ms*	*ms*		*μM*	*μM*
(A) PDAA								
040688.1	0.74	46	13	2.1	9.2	−0.003	21.2	26.1
040688.2	0.98	38	13	2.4	6.2	0.012	12.6	14.9
040788.1	0.81	55	9	2.1	7.5	−0.020	17.0	22.1
050988.1	0.95	38	9	2.3	6.1	−0.043	20.1	25.5
052588.1	0.68	64	19	2.1			23.2	23.7
062388.1	0.95	36	7	2.5	6.0	−0.088	14.7	20.1
062888.1	0.77	34	6	2.4	6.4	−0.082	16.4	19.5
062988.1	0.48	37	7	3.0	6.6	−0.002	12.8	16.0
Mean		44	10	2.4	6.9	−0.032	17.3	21.0
SE of mean				0.1	0.4	0.015	1.4	1.5
(B) DMPDAA								
060487.1	0.44	45	10	3.8	7.5	−0.004	18.8	24.4
061087.1	0.54	54	9	3.5	8.6	0.051	10.9	15.5
071387.1	0.42	60	9	2.7	10.7	0.010	26.4	39.6
071487.1	0.43	46	9	3.2	8.1	−0.097	16.8	23.0
100587.1	0.42	65	18	3.4	8.0	−0.073	21.1	29.0
100987.1	0.53	43	7	2.7	7.2	−0.028	23.3	30.8
101687.1	0.63	65	9	2.4	14.5	0.053	31.5	40.8
102287.1	0.50	46	8	2.7	8.1	−0.020	21.6	28.6
102887.1	0.39	53	7	2.9	8.2	−0.011	20.8	26.4
Mean		53	10	3.0	9.0	−0.013	21.2	28.7
SE of mean				0.2	0.8	0.017	1.9	2.6

A and *B* give results obtained from experiments with PDAA and DMPDAA, respectively. Column *1* gives the fiber reference and column *2* gives the concentration of indicator that was present at the optical recording site when the measurements used for columns *5–9* were made. Columns *3* and *4* give the times that elapsed, respectively, from saponin treatment to the measurement and from indicator addition to the end-pool solutions to the measurement. Column *5* gives the interval between time to half-peak of the action potential and time to half-peak of indicator-related $\Delta A(570)$. Column *6* gives the half-width of the $\Delta A(570)$ signal. Column *7* gives the average value of the $\Delta A(570)$ signal during the period 200–350 ms after stimulation divided by the early peak value; the $\Delta A(570)$ signals were corrected for changes in indicator concentration during the sampling period, as described in Fig. 10. The falling phase of the $\Delta A(570)$ signals from fiber 052588.1 were contaminated by a movement artifact so that reliable estimates of half-width (column *6*) and the steady level (column 7) could not be obtained. Columns *8–9* give peak free [Ca] calculated from peak $\Delta A(570)/l$ and resting $A(520)/l$ as described in Methods; column *8* gives the value calculated on the assumption that all the indicator was able to react with Ca as it does in cuvette calibrations and column *9* gives the value calculated on the assumption that only the freely diffusible indicator was able to react with Ca (see text). Since the value of peak free [Ca] is much smaller than the dissociation constant of PDAA or DMPDAA for Ca, the values in column *9* have been estimated from the values of $(R + 1)$ times the values in column *8*. $(R + 1)$ was not determined in fibers 040688.1 and 100587.1 so that the average values from all the other fibers containing the same indicator were used, i.e., $(R + 1) = 1.23$ for fiber 040688.1 and 1.37 for fiber 100587.1.

9.0 ms with DMPDAA (Table II, column *6*). These values are also simliar to those obtained with tetramethylpurpurate, 7.9 ms (Table III of Maylie et al., 1987*a*, the myoplasmic component), and with antipyrylazo III, 10.1 ms (Table IV of Maylie et al., 1987*c*).

The average values of indicator-related $\Delta A(570)_{steady}/\Delta A(570)_{peak}$ (Table II, column 7) were −0.032 with PDAA and −0.013 with DMPDAA. These values are not significantly different from zero. The value for PDAA, but not that for DMPDAA, is significantly different from 0.01 and 0.02, the limits of the range 0.01–0.02 estimated for $\Delta[Ca]_{steady}/\Delta[Ca]_{peak}$ in intact fibers (Hollingworth and Baylor, 1986; Baylor and Hollingworth, 1988).

Columns *8* and *9* or Table II give two different estimates of myoplasmic peak free [Ca] after a single action potential (see Methods). The estimates in column *8* were calculated on the assumption that all the indicator inside a fiber was able to react with Ca in the same manner as it does in a cuvette calibration; the average values were 17.3 μM with PDAA and 21.2 μM with DMPDAA. The estimates in column *9* were calculated on the assumption that only freely diffusible indicator, equal to the total concentration of indicator divided by $(R + 1)$ (Table I, column *5*), was able to react with Ca. The average values were 21.0 μM with PDAA and 28.7 μM with DMPDAA.

The average values of peak free [Ca] obtained with 0.5–1.0 mM PDAA (Table II *A*, columns *8* and *9*) are slightly smaller than the corresponding values obtained with 2.0–5.2 mM PDAA (page 617). This difference is due to the slight increase in peak free [Ca] that occurred during the first part of four of the eight experiments with PDAA (Fig. 12 *A* and page 617). The average values of peak free [Ca] obtained with 0.4–0.6 mM DMPDAA (Table II *B*, columns *8* and *9*) are essentially the same as those obtained with 1.75–2.25 mM DMPDAA (page 620). Because any uncertainties in the correction of the $\Delta A(570)$ signals for their intrinsic components are likely to be small with large concentrations of indicator, the values of peak free [Ca] obtained with 2.0–5.2 mM PDAA or 1.75–2.25 mM DMPDAA are considered to be more reliable that those given in columns *8* and *9* of Table II.

Dichroic Components of the Absorbance of PDAA or DMPDAA Inside a Fiber

If some of the bound or sequestered indicator molecules inside a fiber were oriented, as might occur if they were associated with the contractile filaments or the SR or some other oriented structure in muscle, the amount of linearly polarized light absorbed by the indicator might depend on the orientation of the plane of polarization. This possibility was investigated by measuring fiber dichroism, $A(\lambda, \delta)$, defined as the absorbance of 0° light minus that of 90° light (Irving et al., 1987). Resting indicator-related dichroism was estimated from the difference $A(520, \delta)$ minus $A(690, \delta)$, which was plotted as a function of indicator-related $A(520)$ and fitted by a straight line of the form $a \cdot A(520) + b$. In eight fibers containing PDAA, the average value of a was 0.0024 (SEM, 0.0051), which is not significantly different from zero. In 12 fibers containing DMPDAA, the average value of a was 0.0065 (SEM, 0.0022), which is significantly different from zero. These values are smaller than those found in cut fibers containing arsenazo III, 0.043 (Maylie et al., 1987*b*);

antipyrylazo III, 0.042 (Maylie et al., 1987*c*); or tetramethylpurpurate, 0.029 (Maylie et al., 1987*a*).

We also looked for the presence of indicator-related dichroic signals $\Delta A(520, \delta)$ and $\Delta A(570, \delta)$ following an action potential. Any such signals were small, with an average amplitude of <2–3% of the Ca signal, and were not studied further.

Ca Signals Recorded during Repetitive Stimulation

Fig. 17 shows pairs of traces, taken with one and ten action potential stimulation at 100 Hz, from a fiber that contained 1.55–1.59 mM DMPDAA (same experiment as

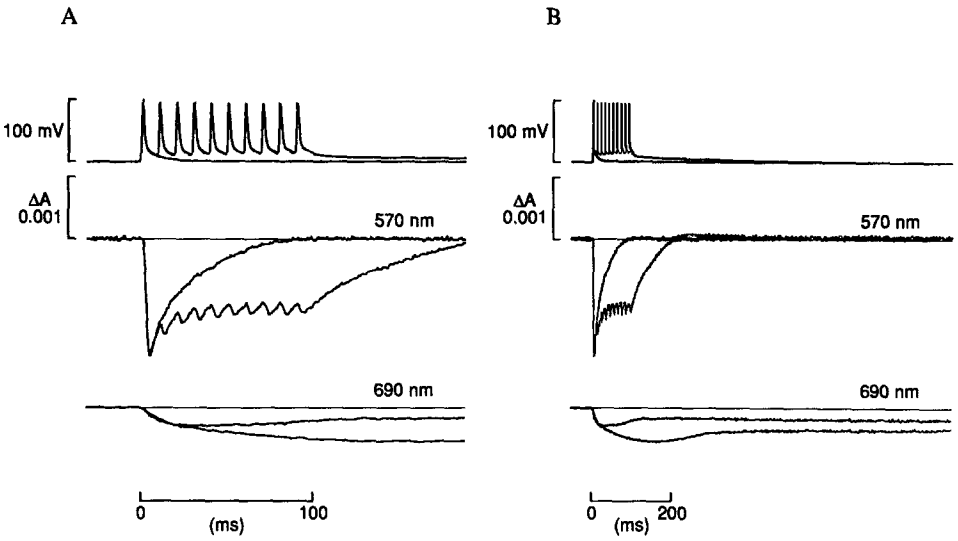

FIGURE 17. Effect of repetitive stimulation on the Ca signal recorded with DMPDAA, from the experiment in Figs. 14–16. The fiber was stimulated to give a single action potential or ten action potentials at 100 Hz. The upper pair of traces in each panel shows the action potentials, the middle pair shows the indicator-related $\Delta A(570)$ signals, and the lower pair shows the $\Delta A(690)$ signals. *A* and *B* are plotted with different time bases. The amplitude of the first action potential was 129 mV; the concentration of DMPDAA was 1.55–1.59 mM; the fiber diameter was 78 μm.

Figs. 14–16). *A* and *B* shows the same traces plotted on a fast and slow time base, respectively. In each panel, the top pair of traces shows the action potential, the middle pair shows the indicator-related $\Delta A(570)$ signals, and the bottom pair shows the $\Delta A(690)$ signals. The $\Delta A(570)$ signal following the first action potential had a peak amplitude of -0.00193, which corresponds to peak free [Ca] = 21.4 μM if all the indicator was able to react normally with Ca. The average value of $\Delta A(570)$ between the seventh and tenth peaks was -0.00129, which corresponds to free [Ca] = 14.2 μM. After stimulation ceased, the $\Delta A(570)$ signals returned to a level just slightly above the prestimulus baseline (Fig. 17 *B* and Fig. 16).

Experiments similar to that in Fig. 17 were carried out on five fibers containing

1.24–2.45 mM DMPDAA and on one fiber containing 1.73–3.07 mM PDAA. The average value of $\Delta A(570)$ between the seventh and tenth peaks was, on average, equal to 0.62 times the value of the corresponding first peak. This ratio is similar to that estimated from results obtained with antipyrylazo III and tetramethylpurpurate, ~0.64 (page 170 in Maylie et al., 1987*a*). If peak free [Ca] following a single action potential is 20–30 μM, as the experiments in this article suggest, the approximately steady level reached during a ten action potential 100 Hz tetanus would be 0.62 times 20–30 μM = 12–19 μM. This range is somewhat greater than that estimated with aequorin in intact fibers, 5–10 μM at 10–21°C (Blinks et al., 1978; Allen and Blinks, 1979; Cannell, 1986).

DISCUSSION

The results presented in this article show that the purpurate indicators PDAA and DMPDAA have two main advantages over tetramethylpurpurate for measuring Ca signals in muscle (Maylie et al., 1987*a*). The first is that their absorbance spectra in resting muscle match their Ca-free cuvette spectra (Fig. 6 and pages 608–609) whereas the tetramethylpurpurate absorbance spectrum matches that of a calibration solution in which 11–15% of the indicator is complexed with Ca. The most likely explanation of this result is that PDAA and DMPDAA, unlike tetramethylpurpurate, are unable to enter the high free [Ca] environment of the SR. We cannot rule out the possibility, however, that some PDAA or DMPDAA enters the SR and becomes complexed with Ca, and that the expected blue shift in the absorbance spectrum produced by Ca complexation is masked by a red shift associated with the indicator's being inside a muscle fiber (pages 609–610).

The second advantage of PDAA and DMPDAA over tetramethylpurpurate is that, after the myoplasmic free [Ca] transient is over, the Ca signal from PDAA or DMPDAA returns to the prestimulus baseline (Figs. 7 *B*, 11, and 14; Table II, column 7; pages 618, 621, and 623), whereas that recorded with tetramethylpurpurate reverses direction and reaches a steady level with an amplitude that is about half that of the early peak. The value of indicator-related $\Delta A(570)_{steady}/\Delta A(570)_{peak}$ obtained with either PDAA or DMPDAA was not significantly different from zero (pages 618, 621, and 623). With PDAA, however, it was significantly different from 0.01 and 0.02, the limits of the range 0.01–0.02 estimated for $\Delta[Ca]_{steady}/\Delta[Ca]_{peak}$ in intact fibers (Hollingworth and Baylor, 1986; Baylor and Hollingworth, 1988). If cut fibers also have a slight elevation of myoplasmic free [Ca] that is maintained 200–350 ms after an action potential, the expected steady $\Delta A(570)$ signal with PDAA may have been offset by an absorbance change of opposite sign. This could arise if some of the PDAA inside a fiber entered the SR (see preceding paragraph) and, after an action potential, underwent a change in absorbance similar to that observed with tetramethylpurpurate. An absorbance change of opposite sign could also arise from a small, consistent error in the procedure used to correct the $\Delta A(570)$ signals for their intrinsic components.

Whatever the reason for the small negative average value of $\Delta A(570)_{steady}/\Delta A(570)_{peak}$ obtained with PDAA, the values of $\Delta A(570)_{steady}/\Delta A(570)_{peak}$ obtained with either PDAA (-0.0068 with 2.0–5.2 mM indicator, page 618; -0.032 with

0.5–1.0 mM indicator, column 7 in Table II *A*) or DMPDAA (0.0032 with 1.75–2.25 mM indicator, page 621; −0.013 with 0.4–0.6 mM indicator, column 7 in Table II *B*) are less in absolute value, by more than one order of magnitude, than those obtained with tetramethylpurpurate, which are ~ −0.5. This is consistent with the idea that tetramethylpurpurate is able to enter the SR but that PDAA and DMPDAA are mostly or entirely excluded, presumably because the two acetic acid groups on each molecule are ionized at neutral pH. Thus, the synthesis of PDAA and DMPDAA appears to represent progress towards the goal to make a Ca indicator that is confined to the myoplasmic solution and has a K_D in the low millimolar range (cf. page 173 in Maylie et al., 1987*a*).

After an action potential in a fiber containing either 2.0–5.2 mM PDAA or 1.75–2.25 mM DMPDAA, the average value of peak free [Ca] was estimated to be the same, 21 μM, with either indicator (pages 617 and 620), if all the indicator inside the fiber was able to react with Ca as in cuvette calibrations. If only freely diffusible indicator was able to so react, the average values were 26 μM with PDAA and 28 μM with DMPDAA. With smaller concentrations of indicator, in which the intrinsic corrections are less reliable, the corresponding range of myoplasmic peak free [Ca] was 17–21 μM with 0.5–1.0 mM PDAA and 21–29 μM with 0.4–0.6 mM DMPDAA (Table II, columns *8* and *9*). The correct value of myoplasmic peak free [Ca] is likely to lie within the range set by these two calibration assumptions, ~20–30 μM, which is similar to the range estimated with tetramethylpurpurate (Maylie et al., 1987*a*). A free [Ca] transient of amplitude 20–30 μM, though only 7–9 ms in half-width (Table II, column *6*), is sufficient to complex ~0.9 of the Ca-regulatory sites on troponin with Ca (see Fig. 11 and page 168 in Maylie et al., 1987*a*) and thereby to allow nearly maximal activation of the thin filaments after a single action potential (Kress et al., 1986).

Purpurate, tetramethylpurpurate, PDAA, and DMPDAA are the only Ca indicators used to date that give values of myoplasmic peak free [Ca] as large as 20 μM, on the usual calibration assumption that the indicator reacts with Ca inside a fiber in the same manner that it does in a cuvette solution. These large values may be related to the fact that purpurate indicators (*a*) have a relatively low affinity for Ca, with K_D's in the low millimolar range, and (*b*) are bound or sequestered to a lesser extent than the other Ca indicators that have been used inside muscle fibers.

There are at least two advantages associated with the use of a low affinity indicator to measure the myoplasmic free [Ca] transient. First, if an indicator's optical signal is to provide a reliable estimate of the spatial average of free [Ca], the optical response at any location should be proportional to local free [Ca]. To ensure that this is the case, the indicator should be distributed uniformly throughout the myoplasm and, at any location, should remain mostly Ca free. This requires that the K_D of the indicator should be at least an order of magnitude larger than the maximal value of free [Ca] attained anywhere in the cell (cf. Scarpa et al., 1978), in which case Eq. 2 becomes $f_{[Ca]} \approx [Ca]/K_D$. According to Cannell and Allen (1984), peak free [Ca] near the SR Ca release sites may be several times the spatially averaged peak value (which we estimate to be 20–30 μM) or ~0.1 mM. Thus, to obtain a reliable estimate of the spatial average of the myoplasmic free [Ca] transient, the K_D of the indicator should be ~1 mM or larger.

Second, if some of the indicator that is bound or sequestered is unable to react with Ca, the error introduced into the estimate of free [Ca] is smaller for an indicator with low affinity than for one with high affinity. Suppose, for example, that 25% of an indicator is bound or sequestered and Ca free, so that only 75% of the indicator is able to react with myoplasmic Ca. If free [Ca] is spatially uniform and has an actual peak value of 30 μM after an action potential, the fraction of free indicator that is complexed with Ca at the time of the peak is (30 μM)/(30 μM + K_D), on the assumption that the reaction between Ca and indicator is sufficiently rapid for Eq. 2 to apply. If a Ca indicator with K_D = 1,000 μM is used, f—the fraction of total indicator that is complexed with Ca—is 0.75 × 30/(30 + 1,000) = 0.0218. If the value of free [Ca] is estimated from f = 0.0218 on the assumption that all the indicator is able to react normally with myoplasmic Ca, Eq. 2 would give peak free [Ca] = 22.3 μM. This estimate is ~25% less than the actual peak value of 30 μM. On the other hand, if an indicator with K_D = 1 μM is used, f = 0.75 × 30/(30 + 1) = 0.726 and Eq. 2 would give peak free [Ca] = 2.65 μM. In this case, the estimate is smaller than the actual peak value by an order of magnitude.

There are also some disadvantages that may arise from the use of low affinity Ca indicators. Any estimate of free [Ca] relies on the measurement of a change in light intensity, ΔI, that occurs when the indicator becomes complexed with Ca. If two hypothetical indicators, one with a low affinity for Ca and the other with a high affinity, undergo the same optical change when Ca is complexed, the same amplitude ΔI signal would normally require a larger concentration of the low affinity indicator than of the high affinity indicator (Tsien, 1980). The use of a large concentration of indicator would be a disadvantage if the indicator were expensive, if it were difficult to introduce into cells, if it had any pharmacological or toxic effects, or if the added osmolarity posed a problem. Another disadvantage could arise if there were some kind of artifactual signal that had an amplitude proportional to resting absorbance, such as might arise in a muscle cell from fiber movement. The amplitude of such a signal would be expected to increase with increasing concentration of indicator. The slight positive component that is present in some of the traces in Fig. 11 (see page 616) may be an example of this kind of artifactual signal.

One clear advantage of tetramethylpurpurate, PDAA, and DMPDAA over other indicators that have been used in muscle is that they are bound or sequestered to a relatively small extent inside fibers. On average, 19% of the intracellular PDAA and 27% of either tetramethylpurpurate or DMPDAA are estimated to be bound or sequestered; these values are given by $100 \cdot R/(R + 1)$ (column *5* in Table I; column *5* in Table II of Maylie et al., 1987*a*). By comparison, Maylie et al. (1987*b*, *c*), using the same cut fiber technique that we used, estimated that 73% of the arsenazo III and 68% of the antipyrylazo III are bound or sequestered. Baylor et al. (1986), using intact frog fibers, estimated the extent of indicator binding or sequestration by comparing the value of the apparent diffusion constant of an indicator with that expected for a molecule of the same size diffusing in cut muscle fibers (Maylie et al., 1987*a–c*) and in skinned muscle fibers (Kushmerick and Podolsky, 1969). With this method, they estimated that the fraction of indicator bound or sequestered was 0.85–0.87 with arsenazo III, 0.74–0.77 with antipyrylazo III, and 0.88–0.89 with azo1. Baylor and Hollingworth (1988), also using the same method on intact fibers,

estimated that 0.60–0.65 of fura-2 is bound or sequestered. Konishi et al. (1988) obtained two other estimates of the fraction of fura-2 that is bound in intact fibers: 0.6–0.7 was estimated from measurements of fluorescence intensity and fluorescence anisotropy, and 0.8–0.9 was estimated from measurements of the shift in the wavelength dependence of the emitted fluorescence. Since sequestered indicator molecules might not appear to be bound in such measurements, the values 0.6–0.7 and 0.8–0.9 represent lower limits of the fractional amount of fura-2 that is bound or sequestered inside a muscle fiber. In contrast to these three different estimates that 0.6–0.9 of the fura-2 inside an intact fiber is bound, Klein et al. (1988) found that little or no fura-2 was bound in their cut fiber experiments. They reported that the equilibrium concentration of fura-2 in the central optical recording site of a cut fiber was essentially the same as that in the end-pool solutions, although the spectral properties of the fura-2 inside the fiber were different from those in calibration solutions. Thus, it appears that 0.7 or more of the arsenazo III, antipyrylazo III, or azo1 inside a fiber is bound or sequestered and that, except for the observation of Klein et al. (1988), at least 0.6 of the fura-2 inside a fiber is bound or sequestered.

Bound or sequestered indicator molecules may not react at all with Ca, as mentioned above, or may react with altered properties. If the affinity for Ca or the optical change produced by its complexation is reduced, the estimate of free [Ca] would lie somewhere between the two extremes of the immobilized indicator molecules reacting normally with Ca or not reacting at all. On the other hand, if the affinity for Ca or the optical change associated with Ca binding is increased, the estimate of free [Ca] would exceed the actual myoplasmic value. Because of these uncertainties concerning the properties of bound or sequestered indicator molecules, it seems highly desirable to use indicators that are minimally bound or sequestered. The purpurate indicators, with PDAA being the best example, appear to meet this goal better than any other absorbance or fluorescence indicators yet used in muscle. Hopefully, other indicators will become available in the future that are neither bound nor sequestered inside muscle fibers, or inside other cells where it is important to obtain a quantitative estimate of free [Ca].

We thank the staff of the Yale Department of Cellular and Molecular Physiology Electronics Laboratory for help with the design and construction of equipment. We also thank Drs. Steve Baylor, Masato Konishi, and Paul Pape for providing helpful comments on the manuscript.

This work was supported by the U.S. Public Health Service grant AM-37643.

Original version received 31 January 1989 and accepted version received 11 April 1989.

REFERENCES

Allen, D. G., and J. R. Blinks. 1979. The interpretation of light signals from aequorin-injected skeletal and cardiac muscle cells: a new method of calibration. *In* Detection and Measurement of Free Ca in Cells. C. C. Ashley and A. K. Campbell, editors. Elsevier/North Holland, Amsterdam. 159–174.

Ashley, C. C., and E. B. Ridgway. 1970. On the relationships between membrane potential, calcium transient and tension in single barnacle muscle fibres. *Journal of Physiology.* 209:105–130.

Baylor, S. M., W. K. Chandler, and M. W. Marshall. 1982*a*. Optical measurements of intracellular pH and magnesium in frog skeletal muscle fibres. *Journal of Physiology.* 331:105–137.

Baylor, S. M., W. K. Chandler, and M. W. Marshall. 1982*b*. Use of metallochromic dyes to measure changes in myoplasmic calcium during activity in frog skeletal muscle fibres. *Journal of Physiology.* 331:139–177.

Baylor, S. M., W. K. Chandler, and M. W. Marshall. 1983*a*. Sarcoplasmic reticulum calcium release in frog skeletal muscle fibres estimated from arsenazo III calcium transients. *Journal of Physiology.* 344:625–666.

Baylor, S. M., M. E. Quinta-Ferreira, and C. S. Hui. 1983*b*. Comparison of isotropic calcium signals from intact frog muscle fibers injected with arsenazo III or antipyrylazo III. *Biophysical Journal.* 44:107–112.

Baylor, S. M., and S. Hollingworth. 1988. Fura-2 calcium transients in frog skeletal muscle fibres. *Journal of Physiology.* 403:151–192.

Baylor, S. M., S. Hollingworth, C. S. Hui, and M. E. Quinta-Ferreira. 1986. Properties of the metallochromic dyes arsenazo III, antipyrylazo III and azo1 in frog skeletal muscle fibres at rest. *Journal of Physiology.* 377:89–141.

Blinks, J. R. 1965. Influence of osmotic strength on cross-section and volume of isolated single muscle fibres. *Journal of Physiology.* 177:42–57.

Blinks, J. R., R. Rudel, and S. R. Taylor. 1978. Calcium transients in isolated amphibian muscle fibres: detection with aequorin. *Journal of Physiology.* 277:291–323.

Blinks, J. R., W. G. Wier, P. Hess, and F. G. Prendergast. 1982. Measurement of Ca concentrations in living cells. *Progress in Biophysics and Molecular Biology.* 40:1–114.

Cannell, M. B. 1986. Effect of tetanus duration on the free calcium during the relaxation of frog skeletal muscle fibres. *Journal of Physiology.* 376:203–218.

Cannell, M. B., and D. G. Allen. 1984. Model of calcium movements during activation in the sarcomere of frog skeletal muscle. *Biophysical Journal.* 45:913–925.

Colquhoun, D., and F. J. Sigworth. 1983. Fitting and statistical analysis of single-channel records. *In* Single-Channel Recording. B. Sakmann and E. Neher, editors. Plenum Press, New York. 191–263.

Crank, J. 1956. The Mathematics of Diffusion. Clarendon Press, Oxford. 347 pp.

Geier, G. 1968. Die Kinetik der Murexid-Komplexbildung mit Kationen Verschiedenen Koordinationscharakters. Eine Untersuchung mittels der Temperatursprung-Relaxationsmethode. *Helvetica Chimica Acta.* 51:94–105.

Hille, B., and D. T. Campbell. 1976. An improved Vaseline gap voltage clamp for skeletal muscle fibers. *Journal of General Physiology.* 67:265–293.

Hirota, A., W. K. Chandler, P. L. Southwick, and A. S. Waggoner. 1988. Calcium transients in frog cut twitch fibers measured with 1,1′-dimethylmurexide-3,3′-diacetic acid. *Biophysical Journal.* 53:647*a*. (Abstr.)

Hollingworth, S., R. W. Aldrich, and S. M. Baylor. 1987. In vitro calibration of the equilibrium reactions of the metallochromic indicator dye antipyrylazo III with calcium. *Biophysical Journal.* 51:383–393.

Hollingworth, S., and S. M. Baylor. 1986. Calcium transients in frog skeletal muscle fibers injected with azo1, a tetracarboxylate Ca indicator. *In* Optical Methods in Cell Physiology. P. DeWeer and B. M. Salzberg, editors. Wiley and Sons, Inc., New York. 261–283.

Irving, M., J. Maylie, N. L. Sizto, and W. K. Chandler. 1987. Passive electrical and intrinsic optical properties of cut frog twitch fibers. *Journal of General Physiology.* 89:1–40.

Jobsis, F. F., and M. J. O'Connor. 1966. Calcium release and reabsorption in the sartorius muscle of the toad. *Biochemical and Biophysical Research Communications.* 25:246–252.

Klein, M. G., B. J. Simon, G. Szucs, and M. F. Schneider. 1988. Simultaneous recording of calcium transients in skeletal muscle using high- and low-affinity calcium indicators. *Biophysical Journal.* 53:971–988.

Konishi, M., A. Olson, S. Hollingworth, and S. M. Baylor. 1988. Myoplasmic binding of fura-2 investigated by steady-state fluorescence and absorbance measurements. *Biophysical Journal.* 54:1089–1104.

Kovacs, L., E. Rios, and M. F. Schneider. 1983. Measurement and modification of free calcium transients in frog skeletal muscle fibres by a metallochromic indicator dye. *Journal of Physiology.* 343:161–196.

Kress, M., H. E. Huxley, A. R. Faruqi, and J. Hendrix. 1986. Structural changes during activation of frog muscle studied by time-resolved X-ray diffraction. *Journal of Molecular Biology.* 188:325–342.

Kushmerick, M. J., and R. J. Podolsky. 1969. Ionic mobility in muscle cells. *Science.* 166:1297–1298.

Maylie, J., M. Irving, N. L. Sizto, G. Boyarsky, and W. K. Chandler. 1987*a*. Calcium signals recorded from cut frog twitch fibers containing tetramethylmurexide. *Journal of General Physiology.* 89:145–176.

Maylie, J., M. Irving, N. L. Sizto, and W. K. Chandler. 1987*b*. Comparison of arsenazo III optical signals in intact and cut frog twitch fibers. *Journal of General Physiology.* 89:41–81.

Maylie, J., M. Irving, N. L. Sizto, and W. K. Chandler. 1987*c*. Calcium signals recorded from cut frog twitch fibers containing antipyrylazo III. *Journal of General Physiology.* 89:83–143.

McMillan, F. H., and H. M. Wuest. 1953. Some xanthineacetic acid derivatives. *Journal of the American Chemical Society.* 75:1998–2000.

Merck, E., O. Wolfes, and E. Kornick. 1922. Verfahren zur Darstellung von Carbonsauren der Purinreihe. *German Patent.* 352:980.

Miledi, R., I. Parker, and G. Schalow. 1977. Measurement of calcium transients in frog muscle by the use of arsenazo III. *Proceedings of the Royal Society, Series B.* 198:201–210.

Miledi, R., I. Parker, and P. H. Zhu. 1982. Calcium transients evoked by action potentials in frog twitch muscle fibres. *Journal of Physiology.* 333:655–679.

Ogawa, Y., H. Harafuji, and N. Kurebayashi. 1980. Comparison of the characteristics of four metallochromic dyes as potential calcium indicators for biological experiments. *Journal of Biochemistry (Tokyo).* 87:1293–1303.

Ohnishi, S. T. 1978. Characterization of the murexide method: dual-wavelength spectrophotometry of cations under physiological conditions. *Analytical Biochemistry.* 85:165–179.

Ohnishi, S. T. 1979. Interaction of metallochromic indicators with calcium sequestering organelles. *Biochimica et Biophysica Acta.* 585:315–319.

Palade, P., and J. Vergara. 1981. Detection of Ca with optical methods. *In* The Regulation of Muscle Contraction: Excitation-Contraction Coupling. A. D. Grinnell and M. A. B. Brazier, editors. Academic Press, New York. 143–158.

Palade, P., and J. Vergara. 1982. Arsenazo III and antipyrylazo III calcium transients in single skeletal muscle fibers. *Journal of General Physiology.* 79:679–707.

Palade, P., and J. Vergara. 1983. Stoichiometries of arsenazo III-Ca complexes. *Biophysical Journal.* 43:355–369.

Rios, E., and M. F. Schneider. 1981. Stoichiometry of the reactions of calcium with the metallochromic indicator dyes antipyrylazo III and arsenazo III. *Biophysical Journal.* 36:607–621.

Rudel, R., and S. R. Taylor. 1973. Aequorin luminescence during contraction of amphibian skeletal muscle. *Journal of Physiology.* 233:5P–6P. (Abstr.)

Scarpa, A., F. J. Brinley, and G. Dubyak. 1978. Antipyrylazo III, a "middle range" Ca metallochromic indicator. *Biochemistry.* 17:1378–1386.

Sims, P. J., A. S. Waggoner, C. H. Wang, and J. F. Hoffman. 1974. Studies on the mechanism by which cyanine dyes measure membrane potential in red blood cells and phosphatidylcholine vesicles. *Biochemistry.* 13:3315–3330.

Southwick, P. L., and A. S. Waggoner. 1989. Synthesis of purpurate-1,1′-diacetic acid (PDAA) tripotassium salt. A new calcium indicator for biological applications. *Organic Preparations and Procedures International.* In press.

Tsien, R. Y. 1980. New calcium indicators and buffers with high selectivity against magnesium and protons: design, synthesis, and properties of prototype structures. *Biochemistry.* 19:2396–2404.